REPUBLIC OF TÜRKİYE

ALTINBAŞ UNIVERSITY

Institute of Graduate Studies

Mechanical Engineering

AERODYNAMIC OPTIMIZATION OF UAV WING DESIGN USING COMPUTATIONAL FLUID DYNAMICS (CFD) ANALYSIS

Ezar Shaban A DHAN

Master’s Thesis

Supervisor

Asst. Prof. Dr. Yaser ALAIWI

İstanbul, 2025

AERODYNAMIC OPTIMIZATION OF UAV WING DESIGN USING COMPUTATIONAL FLUID DYNAMICS (CFD) ANALYSIS

Ezar Shaban A DHAN

Mechanical Engineering

Master's Thesis

ALTINBAŞ UNIVERSITY

2025

The thesis titled AERODYNAMIC OPTIMIZATION OF UAV WING DESIGN USING COMPUTATIONAL FLUID DYNAMICS (CFD) ANALYSIS prepared by Ezar Shaban A DHAN and submitted on 21/01/2025 has been **accepted unanimously** for the degree of Master of Science in Mechanical Engineering

____

Asst. Prof. Dr. Yaser ALAIWI

Supervisor

Thesis Defense Committee Members:

Asst. Prof. Dr. Yaser ALAIWI	Department of Mechanical Engineering, Altınbaş University	__________________
Asst. Prof. Dr. İbrahim KOÇ	Department Mechanical Engineering, Altınbaş University	__________________
Asst. Prof. Dr. Haydar İzzettin KEPEKÇİ	Department of Mechatronics Engineering, İstanbul Gelişim University	__________________

I hereby declare that this thesis meets all format and submission requirements for a Master's thesis.

I hereby declare that all information/data presented in this graduation project has been obtained in full accordance with academic rules and ethical conduct. I also declare all unoriginal materials and conclusions have been cited in the text and all references mentioned in the Reference List have been cited in the text, and vice versa as required by the abovementioned rules and conduct.

Ezar Shaban A DHAN

Signature

DEDICATION

I dedicate this research to my dear parents, whose continuous support and invaluable guidance have been the cornerstone of this achievement; I offer you my deepest gratitude and appreciation. To my supervisor, Asst. Prof. Dr. Yaser Alaiwi, thank you for your wise leadership and unwavering mentorship, which have been a constant source of inspiration and motivation. I also express my sincere appreciation to all the faculty and staff of the Department of Mechanical for their efforts and academic support throughout my studies. To my friends and colleagues who have shared this journey of learning and discovery with me, standing by my side through challenges and triumphs, and to everyone who contributed—even with a word or a smile—to the realization of this work, I dedicate this research in recognition and gratitude.

ABSTRACT

AERODYNAMIC OPTIMIZATION OF UAV WING DESIGN USING COMPUTATIONAL FLUID DYNAMICS (CFD) ANALYSIS

A DHAN, Ezar Shaban

M.Sc., Mechanical Engineering, Altınbaş University,

Supervisor: Asst. Prof. Dr. Yaser ALAIWI

Date: 01 / 2025

Pages: 83

This study presents a comprehensive investigation into the structural and aerodynamic performance of unmanned aerial vehicle (UAV) wings constructed from both traditional and composite materials. Specifically, the research focuses on three material configurations: conventional aluminum, Epoxy Sheet Molding Compound (SMC) reinforced with 65% long glass fibers, and Epoxy E-glass composites. The primary objective is to enhance the aerodynamic efficiency and structural integrity of UAV wings through optimal material selection. A detailed computational analysis was conducted utilizing Computational Fluid Dynamics (CFD) to evaluate aerodynamic forces such as lift and drag across all material cases. This was followed by a one-way Fluid-Structure Interaction (FSI) analysis to assess the structural responses of the wings under realistic flight conditions. Additionally, modal analysis was performed to determine the natural frequencies and mode shapes of the wing structures, identifying critical vibrational modes that could impact flight stability. The CFD analysis provided consistent aerodynamic load data for all material configurations, quantifying the forces acting on the wings. The subsequent FSI analysis offered insights into how each material handled stress distributions, deformation characteristics, and structural strains under operational loads. The results revealed significant differences among the materials in terms of safety factors, deformations, and natural frequency behaviors. Notably, the composite materials outperformed aluminum by exhibiting superior structural strength and reduced weight, leading to higher safety margins and improved resistance to vibrational stresses. Among the composites, the Epoxy E-glass material demonstrated the highest safety factor and the most balanced performance regarding stress distribution and deformation control, indicating its superiority for UAV wing design. This research underscores the critical importance of material selection in UAV design, particularly for wing structures where aerodynamic efficiency and structural durability are paramount. The findings provide valuable insights for future UAV developments, highlighting the potential of advanced composite materials to optimize performance, reduce structural weight, and ensure safer, more reliable operation under varying flight conditions.

Keywords: UAV, CFD, FSI, Composite Material, Aerodynamics, Investigation.

TABLE OF CONTENTS

Pages

LIST OF TABLES

Pages

LIST OF FIGURES

Pages

ABBREVIATIONS

AFRL	:	Air Force Research Laboratory
CAD	:	Computer-Aided Design
CFD	:	Computational Fluid Dynamics
CFRC	:	Carbon Fiber-Reinforced Composites
FEM	:	Finite Element Method
FSI	:	Fluid Structure Interaction
GRP	:	Glass-Reinforced Plastic
MMC	:	Metal Matrix Composite
P/M	:	Powder Metallurgy
PMC	:	Polymer Matrix Composites
UAV	:	Unmanned Aerial Vehicle

LIST OF SYMBOLS

σ_{axial}	:	Axial Stress
C_D	:	Drag Coefficient
C_L	:	Lift Coefficient
F_d	:	Drag Force
A	:	Base Area
E	:	Young’s Modulus
f	:	Natural Frequency
I	:	Second Moment of Inertia
L	:	Lift Force
n	:	Safety Factor
p	:	Pressure.
S	:	Wing Reference Area
v	:	Velocity of Fluid
μ	:	Mass Per Unit Length
ρ	:	Fluid Density

1. INTRODUCTION

1.1 BRIEF BACKGROUND

Unmanned Aerial Vehicles (UAVs), commonly known as drones, are aircraft systems that operate without a human pilot onboard. These vehicles can be controlled remotely or fly autonomously using onboard systems and sensors. UAVs are increasingly used in a wide variety of applications due to their versatility, cost-effectiveness, and ability to access areas that are otherwise difficult or dangerous for manned aircraft. Initially developed for military purposes, particularly for surveillance and reconnaissance, UAVs have rapidly expanded into numerous civil and commercial sectors, including agriculture, disaster management, environmental monitoring, and logistics. UAVs are generally categorized into two main types: fixed-wing and rotary-wing (multirotor) aircraft. Fixed-wing UAVs, resembling traditional airplanes, are designed for endurance and long-range flights, making them ideal for missions requiring sustained, high-altitude surveillance or extensive geographic coverage. In contrast, rotary-wing UAVs, such as quadcopters, provide greater maneuverability and the ability to hover in place, which makes them well-suited for tasks that require precision, such as aerial mapping, photography, and infrastructure inspection. The increasing prevalence of UAVs is closely tied to advancements in propulsion systems, battery technology, and control systems. Modern UAVs are powered by lightweight, high-capacity lithium-polymer (Li-Po) or lithium-ion (Li-ion) batteries, which allow for longer flight durations while maintaining the agility and speed necessary for various applications. Brushless motors, coupled with electronic speed controllers, offer efficient propulsion, further enhancing UAV performance. Additionally, GPS and autopilot technologies have revolutionized UAV operations by enabling precise navigation and autonomous flight, which reduces the need for constant human input and allows UAVs to execute complex missions. The rise of UAVs in non-military sectors has also led to the development of sophisticated sensor technologies, including high-resolution cameras, thermal imaging devices, and LiDAR systems, which are integrated into UAV platforms to collect valuable data for industries such as agriculture, construction, and environmental science. UAVs are employed in precision agriculture to monitor crop health, detect water stress, and optimize pesticide application, while in environmental monitoring, UAVs are used to track wildlife populations, assess deforestation, and survey natural disasters. Despite their growing utility, UAV operations are subject to strict regulatory frameworks to ensure safety and privacy. Regulatory bodies such as the Federal Aviation Administration (FAA) in the United States have established guidelines for UAV operations, including altitude restrictions, certification requirements for operators, and limitations on the use of UAVs in certain airspaces. These regulations are critical for balancing the benefits of UAVs with concerns related to air traffic management, security, and privacy [1].

As UAV technology continues to advance, future developments are likely to focus on increasing autonomy, extending flight durations, and integrating artificial intelligence (AI) for enhanced decision-making capabilities. The ongoing research and development in UAV design, materials, and control systems will further enhance their efficiency and broaden their applicability across diverse fields, making UAVs an integral component of modern technological solutions [1].

Composite materials play a pivotal role in the development and performance enhancement of Unmanned Aerial Vehicles (UAVs). These materials, particularly carbon fiber-reinforced polymers (CFRP) and glass fiber-reinforced polymers (GFRP), are extensively used in constructing key UAV components such as the fuselage, wings, and landing gear. The primary advantage of composite materials is their exceptional strength-to-weight ratio. UAVs made from these materials are lighter yet maintain structural integrity, which significantly enhances their flight performance. Reduced weight means lower energy consumption, allowing UAVs to carry more payload or extend their flight duration. In comparison to traditional materials like aluminum, composites can reduce the overall weight by 15% to 45%, making them ideal for both military and commercial UAVs that require long endurance and high maneuverability. Furthermore, composite materials offer superior resistance to fatigue, corrosion, and impacts, which is crucial for UAVs operating in harsh environmental conditions. For instance, UAVs that experience high-speed impacts with foreign objects like birds benefit from the impact resistance and energy absorption characteristics of composites. Additionally, these materials help reduce vibrations and noise, improving overall stability during flight. Another significant aspect is the flexibility in design that composites provide. With advanced manufacturing techniques, engineers can create complex geometries and optimize the aerodynamics of UAV components, further enhancing their efficiency and reducing drag. This level of design optimization is challenging with conventional materials but is easily achieved with composites due to their moldability and adaptability. In conclusion, the integration of composite materials into UAV manufacturing has led to advancements in endurance, payload capacity, fuel efficiency, and overall structural reliability, making them indispensable in the aerospace industry [2].

1.2 SIGNIFICANCE OF THE STUDY

This study is critical in advancing UAV design by integrating advanced composite materials and cutting-edge simulation techniques to improve performance, durability, and efficiency. With UAVs playing vital roles in military, commercial, and environmental applications, the demand for lightweight, high-strength materials is growing. By replacing traditional aluminum with composite materials like carbon fiber and epoxy glass, the study seeks to reduce weight and enhance structural strength, directly impacting UAV fuel efficiency and maneuverability. The use of Fluid-Structure Interaction (FSI) and Computational Fluid Dynamics (CFD) techniques provides a deep analysis of how UAV wings respond to aerodynamic forces like lift and drag, allowing for precise identification of stress points and predicting potential deformation under various flight conditions. The study's modal analysis further helps prevent structural resonance issues such as flutter, which could jeopardize flight safety. By comparing traditional and composite materials, the research offers valuable data for selecting the most efficient materials for UAVs, influencing future designs for safer, more durable, and versatile aerial systems. This study's findings have the potential to significantly improve UAV development, impacting industries that rely on these technologies.

1.3 PROBLEM STATEMENT

Unmanned Aerial Vehicles (UAVs) have become indispensable tools across a wide range of sectors, including military operations, commercial logistics, and environmental monitoring. Despite their growing importance, traditional UAV wing designs, particularly those constructed from conventional materials such as aluminum, exhibit significant limitations that hinder optimal performance. Aluminum has long been a cornerstone in aerospace engineering due to its strength and durability; however, its relatively high density contributes to increased weight, which adversely affects fuel efficiency, maneuverability, and overall flight dynamics of UAVs.

As the demand intensifies for UAVs capable of extended flight ranges, greater payload capacities, and enhanced fuel efficiency, the shortcomings of aluminum wings become increasingly pronounced. These wings often result in elevated drag forces and reduced agility, impairing the UAV's ability to operate effectively in dynamic and challenging environments. Additionally, conventional materials like aluminum may not provide sufficient resilience against the vibrations and mechanical stresses experienced during high-speed or prolonged flights, raising concerns about structural fatigue and the potential for premature failure.

To address these critical issues, this research proposes the exploration of advanced composite materials—specifically carbon fiber and epoxy glass—for UAV wing construction. These materials are renowned for their superior strength-to-weight ratios compared to traditional metals, offering a promising avenue to reduce weight without compromising structural integrity. The study aims to investigate the integration of these composites into UAV wing designs to alleviate the weight burden and enhance resistance to operational stresses.

By focusing on the application of advanced composites, this research seeks to develop innovative wing designs that significantly improve fuel efficiency, maneuverability, and durability of UAVs. The anticipated outcome is a viable solution that not only overcomes the inherent limitations of traditional materials but also meets the evolving performance demands of modern aerospace applications, thereby contributing to the advancement of UAV technology.

1.4 THESIS OBJECTIVES

1.4.1 General Objectives

a. To enhance the aerodynamic performance of UAV wings by incorporating advanced composite materials.

b. To strengthen the structural integrity of UAV wings, with a particular focus on reducing weight while improving overall efficiency and durability.

1.4.2 Specific Objectives

a. To conduct a comprehensive CFD analysis to assess the aerodynamic forces acting on the UAV wing, focusing on pressure distribution and drag reduction.

b. To perform Fluid-Structure Interaction (FSI) analysis to evaluate the impact of aerodynamic forces on the structural response of the UAV wing, ensuring stability under various operational conditions.

c. To analyze the natural frequencies of the UAV wing through modal analysis, identifying potential resonance issues that could compromise structural integrity during flight.

d. To compare the mechanical and structural performance of traditional materials, such as aluminum, with composite materials like carbon fiber and fiberglass, assessing their impact on weight, strength, and flight performance.

e. To optimize the design of UAV wings using composite materials to achieve a balance between weight reduction and increased aerodynamic efficiency, ensuring the wings can withstand high stresses while minimizing material fatigue.

f. To develop design recommendations for future UAV wing structures, integrating findings from CFD, FSI, and modal analyses to propose materials and designs that enhance both aerodynamic and structural performance.

g. To evaluate the long-term durability and fatigue resistance of composite materials in UAV wings under various flight and environmental conditions, ensuring reliability and safety over extended operational periods.

h. To explore the potential for further material innovations and design improvements in UAV wing construction, contributing to the development of more efficient and high-performing unmanned aircraft.

1.5 SCOPE OF THE STUDY

1.5.1 Study Boundaries

a. Focus on UAV Wing Structure: This research is specifically confined to the analysis of the unmanned aerial vehicle (UAV) wing structure, deliberately excluding other components such as the fuselage and tail assemblies.

b. Exclusive Consideration of Fixed-Wing UAVs**: Only fixed-wing UAV configurations are examined in this study; rotary-wing and other alternative UAV designs are not explored.

c. Emphasis on Aerodynamic Performance and Structural Integrity**: The analysis concentrates on the aerodynamic performance and structural integrity of the UAV wing, with particular attention given to the application of composite materials and their impact on wing design and overall performance.

d. Computational Fluid Dynamics (CFD) and Fluid-Structure Interaction (FSI) Analysis**: The scope of the study encompasses CFD analysis to investigate airflow dynamics around the wing and its effects, as well as FSI analysis to assess the interaction between aerodynamic forces and the wing structure.

e. Limited Material Comparison**: The material comparison is restricted to aluminum, carbon fiber, and fiberglass composites. The study does not include other advanced materials such as nanomaterials or hybrid composites.

1.5.2 Study Limitations

a. One-Way Fluid-Structure Interaction Approach**: A one-way FSI methodology is employed to reduce computational time and resource utilization. This approach means that the structural response does not influence the fluid flow, unlike in two-way FSI systems.

b. Reliance on Simulation Tools Without Physical Prototyping: The research does not involve the physical construction or prototyping of UAV wings. Instead, it relies entirely on simulation tools such as ANSYS Fluent for computational fluid dynamics and static structural analysis.

c. Exclusion of Environmental Factors**: Environmental variables, including extreme weather conditions and the effects of turbulence on wing performance, are not accounted for in this study.

d. Assumption of Ideal Operational Conditions**: The study assumes ideal operational conditions for the UAV, without exploring the effects of wear and tear or material degradation over time.

e. Specific Flight Conditions and Velocities: The computational simulations are performed based on particular flight conditions and velocities, which may not represent all possible UAV operational scenarios.

1.6 THESIS STRUCTURE

Chapter 1: Introduction

This chapter provides an overview of UAVs, their significance, and the research problem. It outlines the study's objectives, significance, and scope, offering a foundation for understanding the research's focus and direction.

Chapter 2: Literature Review

In this chapter, a comprehensive review of previous studies is presented. It covers past research on UAV design, the use of composite materials in aerospace applications, and relevant analysis methods such as CFD and FSI. The chapter highlights gaps in existing literature and establishes the need for further research in this area.

Chapter 3: Methodology

This chapter details the research methods employed, including the computational models and simulation tools used. It explains the CFD analysis setup, the FSI approach, and the material selection for the study. The process for linking fluid dynamics to structural analysis and conducting modal analysis is also discussed.

Chapter 4: Results and Discussions

The results from the CFD, FSI, and modal analyses are presented and discussed in this chapter. It compares the performance of the UAV wing under different material conditions, including aluminum and composite materials, highlighting key findings such as drag, lift, stress distribution, and natural frequencies.

Chapter 5: Conclusion and Future Work

This final chapter summarizes the research findings and provides a conclusion on the effectiveness of using composite materials for UAV wing design. It also discusses the limitations of the study and suggests areas for future research, such as exploring Two-Way FSI or additional materials for further optimization.

2. LITERATURE REVIEW

A previous study focused on the production and testing of a UAV built from composite materials. The research described the construction process for durable, lightweight UAVs and assessed the flight performance of such composite aircraft. Fiberglass composites were the primary construction material. The process began with shaping the aircraft using Styrofoam, followed by applying resin and fiberglass to one side of the form. Flight test data demonstrated the aircraft's remarkable stability and strength, particularly in terms of pitch and roll [3].

A master's thesis discussed the development of an automatic landing system for fixed wing unmanned aerial vehicles. This system conducted automatic landings using location information computed by image-processing algorithms. A Ground Control Station program, developed using GCS software, sent commands to the autopilot for landing performance analysis, changing the location data source, or activating/deactivating pilot functions. The system was successfully tested in various flight environments and under different turbulence and wind conditions, demonstrating the aircraft's automatic guidance capabilities [4].

A previous investigation explored the composite structures and material strength of a Belly-Landing Mini UAV. The research involved designing and developing the UAV's fuselage using two-layer sandwich structures made from epoxy resin and composite materials. Three distinct forms of tensile test samples and strength test samples were fabricated according to standards. Findings showed that carbon and glass fibers mixed with epoxy resin demonstrated excellent tensile strength and Young's modulus. Stress simulations using Inventor software yielded promising results, suggesting a highly safe design. Flight trials confirmed the aircraft's success in both maneuvering and take-off tests [5].

Previous research discussed a control device for a small, fixed-wing UAV designed to maintain a specific flight path in turbulent wind conditions. The controller's primary objective was to compensate for wind impact and maintain the intended flight trajectory, which was theoretically confirmed to be globally asymptotically stable. Multiple simulations were conducted to assess the controller's performance. The results showed that the composite controller, incorporating a disturbance observer, was stable and aligned well with the theoretical analysis. Initial flight trials yielded positive results within acceptable parameters when the controller was tested [6].

Different research undertook the exploration, optimization, and design of a fixed-wing structure for an unmanned aircraft. A comparative analysis was carried out among various types of wings, specifically the Beam type, Multi-Ventral-Plate, and Single Block Type. After simulating under specific conditions, including a drag force of 50 Newtons and a lift force of 100 Newtons, the Beam type was concluded to be the superior choice. This suggested potential enhancements to the fixed-wing UAV's design due to its efficiency [7].

A research study investigated the use of a fixed-wing unmanned aerial vehicle (UAV) for mapping semi-undulating terrain. The study evaluated a slope-mapping technique called photogrammetry. The UAV captured images from an altitude of 300 meters. All collected images were analyzed using photogrammetry, also known as Digital Orthophoto and Digital Elevation Model (DEM). The results showed a root mean square (RMS) error of 0.259 for length analysis and 1.169 for slope, demonstrating the effectiveness of this mapping approach [8].

A previous study focused on the impact of vibration on composite materials used in UAV wings. The research compared the modal characteristics of the wing in two configurations: vertically mounted for shaker-table testing and attached to a suspended UAV to simulate a free setup. Sixteen biaxial accelerometers were installed on both wings to measure vibrational characteristics, including natural frequencies, associated modes, and damping coefficients. This accelerometer arrangement allowed data collection both inside and outside the plane to determine the shape of the situation. The shaker-table method produced significantly larger and cleaner signals compared to data acquired from a complete UAV configuration [9].

An earlier study proposed an analytical framework for a drone model to simulate the flight dynamics of a fixed-wing aircraft, integrated into the DATCOM software's dynamic model. The researchers created an experiment-based model using flight test data, which was refined using a Kalman filter to validate the analytical model. Comparison of the two systems revealed that they produced dynamic models with similar characteristics [10].

A previous study examined the properties, rigidity, and strength of a carbon composite wing for an unmanned aircraft. The lightweight wing featured multiple ply patterns with varied spars of different wall thickness dimensions and laminates, as well as sandwich skins with a foam core. To properly load the wing under pull-up maneuver conditions, researchers designed and employed a three-tiered whiffletree system. Multiple deflection and strain gauges measured the wing's static response at various chordwise and spanwise locations. Finite element simulations closely aligned with experimental observations of deflection and stress, indicating the wing's substantial strength despite its light weight [11].

Other studies used SOLIDWORKS software to simulate composite materials for unmanned aircraft. These studies first examined the general properties of composite materials, then numerically analyzed two specific types: laminates and sandwich composites. The research highlighted differences in primary pressures (P1 and P3) and displacement values within the analyzed structures under consistent boundary conditions. Additionally, the studies detailed the progression of the manufacturing process [12].

A comprehensive study of design standards for an Unmanned Aerial Vehicle (UAV) system, specifically targeting a loiter munition UAV, was conducted in previous research. This UAV system was designed to feature day and night functionality, a flight time between 2-3 hours, and the capacity for catapult launch. The UAV was conceived to be compact, easily navigated via a personal Global Positioning System (GPS), and fitted with cutting-edge avionics, making it ideal for defense and border patrol activities. The UAV's structure, characterized by a mid-wing, dual-tail, and a relatively light frame, was found to provide stability across three axes. The research concluded that this design not only assures the UAV's steadiness but also offers notable cost benefits during operations [13].

A subsequent study narrated the process of designing, analyzing, and fabricating a composite frame structure for an unmanned aircraft. The structure comprises a lattice composite structure created using a 3D printer that operates with continuous carbon fiber, and two matrix materials, one being a thermoset. The study outlined the 3D printing process and the finite element analysis of the structure. The analysis results demonstrated a considerable correlation between the experimental data and the theoretical predictions [14].

A previous study focused on simulating a tubercle leading edge for an unmanned aircraft's composite wing using finite element methods. The design phase utilized SOLIDWORKS software, while ANSYS software was employed for developing the finite element model. The research aimed to measure the impact of deformation and stresses on the composite wing of an unmanned aerial vehicle, particularly the tubercle at the wing's leading edge. Two varieties of composite materials were explored: the reinforced rib and the monocoque-foam. Post-analysis results revealed that the monocoque-foam significantly outperformed the reinforced rib, reducing deformation by 50.72% and stress by 35.88% [15].

A comprehensive method for the initial design of aircraft was presented, emphasizing the use of one-way fluid-structure interaction (FSI) in aircraft design. The primary objective of the research was to refine the wing shape of an unmanned aerial vehicle (UAV) to achieve minimal cruise drag. The study focused on design factors such as the wing's taper ratio and dihedral angle, with the UAV's cruise drag as the target outcome. By employing Fluid-Structure Interaction (FSI) analysis and optimization techniques, the researchers successfully reduced the aircraft's drag by 6.3%. The prediction model, developed using the Kriging method, demonstrated a 2.7% deviation in estimating the lowest drag. These findings underscored the value of FSI analysis in improving UAV design for enhanced aerodynamic efficiency [16].

A previous research paper concentrated on the meticulous task of enhancing wing designs for long-endurance unmanned aerial vehicles (UAVs). This scholarly work emphasized the importance of using Fluid-Structure Interaction (FSI) analysis in conjunction with the Kriging method. The study's primary goal was to identify the most aerodynamically efficient wing shape with a high aspect ratio, resulting in minimal aerodynamic drag during UAV cruise conditions. To facilitate this complex optimization process, the research team employed a specialized design optimization tool called PIAnO. This software integrated seamlessly with proprietary codes for simulation and optimization, serving multiple functions: generating various wing geometries, enabling efficient information transfer between different design stages, and accurately identifying the optimal wing shape based on set criteria. Upon completing their rigorous analysis, the researchers discovered that the most optimal wing configuration achieved a noteworthy 5.95% reduction in aerodynamic drag compared to the initial baseline wing design. This study provides valuable insights and a practical approach to significantly improving the aerodynamic efficiency of long-endurance UAVs [17].

Another study shed light on the application of composite materials in unmanned aircraft construction. The research primarily focused on the experimental characterization of a polymer matrix composite laminate, which incorporated an epoxy resin system reinforced with graphene oxide (GO) and fiberglass. Upon reviewing the experimental results, it was observed that EPWM12 outperformed other laminates in terms of maximum tensile strength and ultimate tensile strength. The incorporation of graphene notably strengthened the epoxy composite, resulting in a 4.3% increase in the elongation value compared to conventional epoxy. Moreover, the Young's modulus of the epoxy composite was found to be approximately 66% greater than that of regular epoxy, representing nearly a fourfold increase. These findings highlight the significant improvements in material properties achieved through the use of graphene-reinforced composites in unmanned aircraft construction [18].

A past article highlighted the increasing significance of unmanned aerial vehicles (UAVs) due to their cost-effectiveness and versatility. However, it identified a gap in design techniques that integrate both aerodynamic and structural evaluations for UAV propellers. The study proposed a novel approach to aerodynamic propeller design, utilizing advanced tools and parameters, combined with a structural assessment technique using the Finite Element Method (FEM). Various propeller designs were explored using BEMT and MIL techniques. The finalized design underwent comprehensive numerical tests, combining aerodynamic forces with structural design through Fluid-Structure Interaction (FSI) in ANSYS 18. Aerodynamic assessment showed close alignment between BEMT and CFD results, with minimal deviation. Some propeller designs exhibited superior thrust production. The research's primary accomplishment was developing a design technique for UAV propellers aimed at predicting their efficiency and optimal designs in the initial stages [19].

An in-depth study focused on designing a medium-range fixed-wing unmanned aerial vehicle (UAV) capable of carrying a 25 kg payload. The wing design underwent Fluid-Structure Interaction (FSI) analysis to verify and enhance its aerodynamic properties. The study emphasized the value of FSI simulation as a cost-effective and quick method for evaluating aircraft performance, eliminating the need for repeated tests. The project involved defining flight criteria, examining similar UAVs, and using a cyclical estimation method to determine the UAV's total takeoff weight. After evaluating multiple airfoils, the Wortmann fx-76-mp-140 was chosen for the wing. A 3D model of the wing structure was developed using SOLIDWORKS, with design confirmation through XFLR5 and FSI analysis. The FSI analysis, conducted in ANSYS, provided insights into lift-to-drag ratio, wing deformation, and stress. After testing various configurations of dihedral angle, chord length, and wingspan, the study concluded that extending the wingspan from 4.61 meters to 5.11 meters resulted in a 4.9% improvement in the lift-to-drag ratio [20].

Previous research examined the integration of the nonlinear structural tool MSC Nastran into a concurrent programming environment called FlowSimulator. The primary objective was to facilitate fluid-structure interaction (FSI) assessments by combining fluid and structural analysis tools. The study presented a module-based framework where MSC Nastran acts as a central server, communicating with other modules through an XML-RPC server. This setup ensures smooth data transfer and coordination during joint analysis. The research emphasized the importance of MSC Nastran's OpenFSI interface, which allows for the integration of real displacement states from the fluid tool and the collection of resulting loads for structural evaluation. Two main examples were highlighted: one demonstrating a beam-like action becoming rigid due to significant deflections and rotations, and another showing surface buckling on a slender-walled wing structure, influencing overall rigidity and nearby airflow. Both examples revealed the limitations of traditional linear theory in identifying these nonlinear behaviors [21].

A study addressed the evaluation of engine lifespan, focusing on fatigue estimation in unmanned fixed-wing aircraft. It presented a systematic approach to forecast the lifespan of these engines, referred to as "gray color," particularly those operating in high-stress conditions. The research utilized gray prediction models, drawing on output power decay data over a span of 50 flight hours. Results indicated that under typical operation, the engine's power decreases to 9.4 kilowatts after 100 hours, below which the aircraft cannot complete its journey adequately. For high-stress scenarios, the predictive models leveraged degradation data accumulated over 70 hours. The study concluded with a comparative analysis of the predictive results and methodology against alternative approaches such as autoregression, determining that the gray prediction method was more precise in estimating engine lifespan [22].

Prior research examined the design process of an unmanned aerial vehicle using CATIA V5 software. The study then analyzed the aircraft's performance using ANSYS and XFLR software, providing insights into the aerodynamic properties of the UAV's fixed wing. The goal was to enhance the aircraft's aerodynamic design. To extend flight duration and achieve maximum altitude, the most favorable glide ratio was calculated. Simulations were conducted using a Mach number of 0.04202, approximately 14.3 meters per second. The aircraft's construction utilized composite materials such as glass and carbon fibers [23].

A previous study conducted a structural analysis of an unmanned aircraft's composite material wing using the finite element method and ANSYS software. The research investigated and compared various laminates on the wing surface and explored the benefits of structural elements like ribs and spars. Simulation revealed data on deformation, resistance, and potential failure under defined conditions. Results indicated that optimal load reduction was achieved by varying the distributed load along the pressure center. The most effective surface lamination was found to be (45/0/0/45) using carbon fiber fabric, leading to a maximum displacement of 15.27 mm. The introduction of a spar reduced maximum displacement by 29.7%, while ribs did not significantly affect the structural response [24].

Prior research demonstrated that inflatable wings could significantly enhance the portability of small Unmanned Aerial Vehicles (UAVs). The study explored a foam-inflated wing concept, combining rigid and flexible components to potentially reduce packing and logistical requirements before small UAV deployment. Flexible polyester-film materials were used for spars and wing skin construction to minimize packing volume. Cylindrical spars were rigidified using expanding foam for deployment, enhancing buckling resistance. Pre-affixed rigid ribs ensured high shape compliance for the external skin. The solid rib configuration meant the wing's chord length determined the maximum pre-inflation packing dimension. Testing showed the hybrid wing's inflation process was straightforward and rapid. The resulting foam-inflated structure was lightweight and adaptable to anticipated loads. Fundamental ribs maintained high aerodynamic performance despite the wing's inflatable characteristics. Flight testing verified the practicality of this hybrid wing structure concept [25].

A previous paper explored possibilities for simulating composite materials in SOLIDWORKS, along with various aspects of unmanned aerial vehicle (UAV) design and manufacturing, using a real airplane model from the Air Cargo Challenge 2013 competition. The paper initially discussed different types of composite materials, their mechanical properties, and structures. It depicted the UAV wing design process as a multi-phase task. The subsequent section included numerical analysis of two composite structure types: laminates and sandwich composites. The study highlighted variations in displacement and primary stress values (P1, P3) in these structures under identical boundary conditions. The article concluded by elaborating on the manufacturing process development [26].

A previous paper proposed a terminal guidance control for small fixed-wing unmanned aerial vehicles (SUAVs) with wingspans around 1.5 m, utilizing a visible light strap-down seeker. The system was implemented using inexpensive, open-source components costing less than $2000. It demonstrated feasibility, adaptability, and effectiveness for various SUAV types, delivering commendable terminal guidance accuracy (circular error probable = 1.5 m) against a stationary ground target. The study examined the practical median flow algorithm for target tracking, the attitude pursuit guidance law for terminal guidance control, and the pursuit image frame method for large delay interception. Laboratory tests and field flight trials on two different SUAV platforms assessed the system's performance and robustness. This paper offers a reliable, efficacious, and tested reference for the evolution of aggressive SUAVs for SUAV swarms [27].

One of the previous papers aimed to provide guidance through the intricate procedures of designing, producing, and examining an electrically propelled, radio-guided aircraft. The goal was to create an aircraft capable of successful take-off, cruising, safe landing, and bearing the maximum achievable payload. The comprehensive process included design, structural assessment, performance appraisal, material selection, manufacturing, and testing. The final model had an empty weight of 15.43 lbs and a maximum take-off weight of 33.07 lbs. The aircraft featured a wingspan of 70.1 inches, a cruising speed of 46 feet per second, and a top speed of 78 feet per second. The total distance required for take-off was recorded as 100 feet [28].

A previous study rapidly computed design variables to meet strength and stability conditions, the primary verification parameters for composite wing structure, using a genetic algorithm.

An optimization process for variable stiffness stacking, suitable for aircraft wing structure design, was developed. The study proposed an optimization strategy based on laminate parameters, considering the stiffness features of two-dimensional elements as design variables. When compared with optimization results using continuous stiffness optimization as a process function of laminate sequences with genetic algorithms, a sensible stiffness distribution was achieved that complied with crucial guidelines for individual composite layup designs. The stiffness optimization design results were enacted as a finite element model and validated through NASTRAN. The functionality of the stiffness optimization process was demonstrated by achieving outcomes satisfying defined response conditions, such as strength and stability, across multiple wing design areas [29].

Previous research focused on the aerodynamic analysis of unmanned aerial vehicles (UAVs) moving in groups. The study emphasized the importance of understanding how UAVs interact when flying in close proximity. Using computational fluid dynamics, models of a UAV and its propellers were designed, and changes in turbulence, pressure, and speed were investigated. The research found that the movement of one UAV in a flock could affect another, potentially causing unstable motion due to aerodynamic effects from nearby drones. The study concluded that maintaining a certain distance between drones in groups is crucial to reduce these aerodynamic effects. For independently operating UAVs, the importance of recognizing and managing their distance from other UAVs was highlighted, suggesting a need for UAV models to establish their own safe aerodynamic zones [30].

A previous study investigated the strength and stiffness characteristics of a carbon composite wing belonging to an ultralight unmanned aerial vehicle. The wing consisted of foam-core sandwich skins and multiple spars with distinct laminate ply patterns and wall thickness dimensions. A three-tier whiffletree system was designed and used to load the wing under pull-up-maneuver conditions. Multiple strain and deflection gauges recorded the wing's static response at various spanwise and chordwise locations. The wing was incrementally loaded beyond limit and design ultimate loads until structural failure occurred. A geometric nonlinear finite element model was developed, accounting for variations in laminate geometry and adhesively bonded joints. The study found strong alignment between experimental observations and finite element simulations for strain and deflection predictions. Despite its lightness, the wing exhibited exceptional robustness, with a strength-to-weight ratio exceeding 40 at the point of failure [31].

This previous research focused on the structural design methodology for an Unmanned Aerial Vehicle's wing, effectively employing computational methods. The strength and stiffness examination of the UAV wing was accomplished using ANSYS, an FEA software. The existing CAD model and aerodynamic CFD analysis of the vehicle served as design inputs. Aerodynamic loads were applied to the structure as pressure functions using a novel methodology harnessing Artificial Neural Networks. The study also examined potential effects of variations in geometry, material, and lay-up to identify the optimal combination for superior strength and stiffness while minimizing weight and cost. The final design featured a wing with two spars and an entirely composite structure. Compared to a similar aluminum wing, this design was lighter in weight and had adequate strength to withstand all in-flight load conditions and safety factors [32].

Previous research detailed the procedure of a UAV wing's structural design, assessment, and optimization for weight reduction. The study developed an optimized semi-monocoque wing structure, including ribs, spars, and skin, focusing on minimizing weight without compromising the strength-to-weight ratio. Initially, a NACA 2412 airfoil was used to design a solid wing surface. Computational Fluid Dynamics (CFD) analysis was then performed to obtain pressure distribution across various wing configurations by adjusting attack angles. The CFD outcomes were used to determine variations in lift coefficient for distinct attack angles. For structural examination, pressure fields from the CFD analysis were applied to the structural components. The wing was optimized through consideration of multiple scenarios to achieve targeted performance. The optimized wing design resulted in reduced wing weight and increased strength-to-weight ratio, showing notable advancement compared to the standard model [33].

A previous thesis documented the development of the wing structure for a UAV known as Skywalker X8. The project involved engineering a wing box structure twice as large as the existing model, utilizing eco-friendly technology and lightweight materials. Forces acting upon the UAV were modelled and assessed using Star CCM+, a Computational Fluid Dynamics (CFD) software. Alterations to the Computer-Aided Design (CAD) model and Finite Element Method (FEM) simulations were executed in Siemens NX. Eight combinations of five materials (carbon fibre reinforced polymer, low-density polyethylene, polyethylene, polypropylene, and balsa wood) were tested. The most effective combination used polypropylene for the wing skin and balsa for the honeycomb structure. This design, weighing 3.576 kg, yielded specific stress levels at various angles of attack. A Gurney flap was added to the trailing edge to explore potential lift-to-drag ratio improvements, but it did not provide the anticipated enhancements [34].

A previous study highlighted the challenges of designing a high-altitude mini-Unmanned Aerial Vehicle (UAV), focusing on aerodynamic aspects. The mini-UAV under evaluation was a 2 kg class, high-wing, T-Tail configuration. The study conducted a comparative analysis of various high-lift airfoils, demonstrating that selecting an appropriate airfoil for high-altitude use is crucial in the design process. The research showed that the wing loading of a high-altitude UAV is not solely dependent on air density variations. The selected high-lift, low Reynolds number airfoil had a marginal impact on aerodynamic parameters (Cl and Cd) with fluctuations in the Reynolds number. The paper also discussed performance variations caused by operating at off-design conditions, such as sea level [35].

Another study focused on the conception, examination, and creation of a hand-launch, fixed-wing unmanned aerial vehicle (UAV) capable of carrying a 0.8 kg payload. The design procedure involved conceptual, preliminary, and detailed planning. The study included an exploration of aerodynamic properties over the wing to improve the UAV's aerodynamic design, aiming to estimate the optimum gliding ratio for extended flight mission and maximum altitude. The simulation was conducted for subsonic flow with a Mach number of 0.04202 (14.3 m/s). The UAV was manufactured using composite materials including 1mm and 2mm thick glass fiber, 2mm thick carbon fiber, and a carbon rod to attach the empennage to the fuselage. The detailed design was completed in CATIA V5, and the wing analysis was executed using XFLR and ANSYS (fluent) [36].

A previous research aimed to validate the performance of a wing by analyzing its internal structure under maximum lift and inertia force. The study examined the wing's reciprocating motion in a stroke to estimate its peak speed and inertia force load when combined with a reciprocating driver. A 3D computational fluid dynamic (CFD) analysis was performed at the highest angle of attack (AoA) and identified maximum speed to determine the maximum lift and drag. Finite element analysis (FEA) results showed acceptable stress levels, indicating the wing structure's safe load-bearing capacity. This could certify the wing's suitability for incorporation into the RA UAV module [37].

A previous study proposed a methodology for modeling the nonlinear flight dynamics of BPPT Wulung, a fixed-wing UAV, under varying flight altitude and airspeed conditions. This was an initial step towards designing a nonlinear adaptive controller. The model utilized 10 degrees-of-freedom (DOF) differential equations configured as strict-feedback systems, separating the elements of elevator, aileron, rudder, and throttle from the model. The simulation outcomes revealed the behavior of the Wulung UAV's flight dynamics and corroborated the results with real flight test data [38].

A prior article presented an innovative approach using artificial neural networks (ANN) to apply aerodynamic pressures on unmanned aerial vehicles (UAVs) during their design phase. The research aimed to enable seamless fluid-solid interaction for UAV structural design. Computational Fluid Dynamics (CFD) was used to integrate aerodynamic forces into the UAV's steady-state static design using finite element (FE) analysis. To address meshing technique disparities between CFD and FE tools, the researchers developed a method using ANNs to formulate precise pressure functions. After training the ANN with aerodynamic data, these functions determined the UAV's structural strength and rigidity. The study demonstrated that ANNs outperformed conventional 3D regression methods in accurately replicating the aircraft's pressure profile [39].

A comprehensive study was conducted to understand the response of different composite materials when subjected to impact forces. The research emphasized that the precision of numerical simulations depends significantly on well-defined boundary conditions, such as accurate loading conditions and pure mechanical attributes. The study focused on impact assessment of Carbon, Glass, and Kevlar fiber composites using FSI analysis. Ansys Design Modeler was used for creating conceptual designs, while composites were crafted with the ACP tool. The main aim was to identify the most suitable material for impact-intensive tasks. Findings suggested that specific composites, notably those derived from Carbon and S-Glass Uni-Directional fibers, were best suited for addressing impact-related challenges, particularly in areas like Unmanned Aerial Vehicles (UAVs) [40].

A previous study explored methods for simulating the nonlinear dynamics of fixed-wing UAVs under varying airspeed and flight altitude conditions, aiming to develop a nonlinear adaptive controller. The model comprised a 10-degree of freedom differential equations system, separating the aileron, throttle, rudder, and elevator conditions from the constructed model. Simulations revealed the flight dynamics behavior of the Wulung UAV, the study subject. The simulation results closely matched data from actual flight tests [41].

This study examined aerodynamic adjustments to the RQ-7 Shadow's wing, scrutinizing the implications of modifying wing design elements such as airfoil, shape, aspect ratio, and winglet addition during ascent and acceleration stages. A primary goal was to determine the viability of high-lift airfoils like the EPPLER 559 for slower UAV applications. Using ANSYS FLUENT, five unique wing designs underwent Computational Fluid Dynamics simulations. Results showed that the EPPLER 559 airfoil provides enhanced lift at reduced angles of attack compared to the NACA 4415 airfoil, but its advantages diminish as the angle of attack increases. The research concluded that while the EPPLER 559 airfoil is promising for slower UAV uses, its efficiency depends on specific adjustments in wing design elements [42].

Prior research conducted a detailed analysis of flapping wing mechanics for Unmanned Air Vehicles (UAVs), addressing the growing need for compact UAVs in challenging environments like urban settings. The study focused on creating and validating a computational fluid dynamics (CFD) tool that combined a fluid-structure interaction (FSI) solver with vehicle control algorithms. This unified method aimed to forecast the efficiency of a sample flapping wing UAV. Nature-inspired wings, built with carbon fiber frameworks and flexible Mylar membranes, were studied. The combined solver was verified against standard scenarios, demonstrating its reliability and promise. Early simulations of pitch control movements showed that the vehicle could return to the desired position in just three wing flaps [43].

3. METHODOLOGY

This chapter provides a detailed look at fluid dynamics and its many practical uses. It starts by explaining the basic principles of aerodynamics and how they influence technology in different industries. The chapter then moves on to Computational Fluid Dynamics (CFD), showing how important it is for understanding and analyzing fluid flow. Key developments, challenges, and fundamental equations like the Continuity and Navier-Stokes equations are explained clearly, with a focus on their role in simulating fluid behaviour. The concept of Fluid-Structure Interaction (FSI) is also introduced, highlighting its importance in examining how structures and fluids interact, both around and within the structure. The chapter gives special attention to flow-induced instabilities and their relevance in engineering problems. To demonstrate these concepts, the chapter concludes with a case study on the XQ-58A Valkyrie. This case study shows how design principles, aerodynamics, and computational methods are combined. It discusses the use of CAD tools in the design process, along with the CFD and FSI analyses, offering insights into the development and evaluation of advanced UAVs. By the end of this chapter, readers will have a clear understanding of fluid dynamics, its computational aspects, and how these are applied in real-world scenarios, as well as the ongoing developments in the field.

3.1 FLUID MECHANICS

3.1.1 Introduction

Fluid mechanics is the science that studies fluids, both in motion (fluid dynamics) and at rest (fluid statics). Fluids, whether liquids or gases, differ significantly from solids due to their inability to resist shear stress when in a static state. Instead of resisting, fluids continuously deform under the application of shear stress. These characteristic forms the basis of fluid mechanics, which has extensive applications across various fields, from industrial machinery like turbines and pumps to natural phenomena like blood flow and air currents. The study of fluid mechanics involves balancing both theoretical and experimental approaches. Since fluid flow is governed by the principles of mechanics, theoretical models are used to analyze fluid behavior based on the laws of conservation of mass, momentum, and energy. These models, while grounded in established laws, are often simplified for practical purposes because solving them in complex situations can be mathematically challenging. For instance, the geometry of objects and the viscosity of the fluid can significantly complicate these equations. In real-world scenarios, viscosity plays a key role in fluid behavior. It is responsible for energy dissipation in fluid motion, making the analysis more difficult. While some situations allow for the simplification of the equations by neglecting viscosity, most practical fluid flows are viscous. This is particularly true for turbulent flows, where viscosity destabilizes the flow, leading to irregular and chaotic motion. Understanding and estimating turbulent flows often require a combination of experimental data and theoretical models. Another fundamental aspect of fluid mechanics is the study of flow patterns, which are commonly visualized using streamlines, path lines, or streamlines. These flow patterns help describe the behavior of fluids in various conditions, such as laminar (smooth) or turbulent (chaotic) flows. The analysis of these patterns, along with the governing equations, allows for the prediction of forces acting on objects moving through fluids, such as lift and drag on an aircraft or UAV, making this science crucial for designing efficient aerodynamic structures [44].

3.1.2 Fundamental Concepts

a. Fluids as a Continuum:

In fluid mechanics, fluids are treated as a continuum, meaning that properties such as density, pressure, and temperature are assumed to vary smoothly and continuously across space and time. Although fluids are composed of molecules on the microscopic level, the macroscopic approach assumes that these molecules are uniformly distributed, allowing for the use of differential equations to analyze fluid flow. This assumption holds true in most engineering applications except in cases involving microscopic or molecular-level analyses [44].

b. Fluid Properties:

The behavior of fluids under different forces or environmental conditions is determined by several key properties [44]:

Density (ρ): Density is the mass per unit volume of the fluid. In liquids, density is nearly constant, while in gases, it can vary significantly with changes in pressure and temperature. Density is used directly in governing equations to analyze fluid flow.

Pressure (p): Pressure is the force exerted by a fluid on a surface per unit area. It is one of the most important variables in describing fluid behavior and increases with depth in a fluid due to the weight of the fluid above it in a gravitational field.

Viscosity (μ): Viscosity represents a fluid's resistance to deformation or flow. Fluids with high viscosity (e.g., honey) resist flow more than low-viscosity fluids (e.g., water). Viscosity plays a crucial role in determining flow characteristics, particularly near solid surfaces where the no-slip condition applies, meaning the fluid velocity at the surface is zero.

c. Reynolds Number

The Reynolds number is a key dimensionless parameter in fluid dynamics that significantly impacts aerospace applications. For instance, micro air vehicles operate in a low Reynolds number regime (Re < 100,000), which is vastly different from conventional aircraft that operate at Reynolds numbers in the millions. This difference is important because at low Reynolds numbers, airfoils typically experience laminar flow, leading to phenomena like laminar separation bubbles near the leading edge. These bubbles cause a reduction in lift and an increase in drag. Additionally, for objects such as spheres in a flow, drag is primarily influenced by flow separation, with the drag coefficient showing notable changes depending on the Reynolds number. In hypersonic vehicles, the Reynolds number also affects the lift-to-drag ratio, as these vehicles tend to experience large laminar flow regions due to delayed turbulence transition at high Mach numbers. The Reynolds number can be calculated using the following equation [45].

Where:

$$Re = \frac{\rho V L}{\mu} \tag{3.1}$$

ρ : Air density

V : Object velocity

L : Characteristic length

μ : Dynamic viscosity

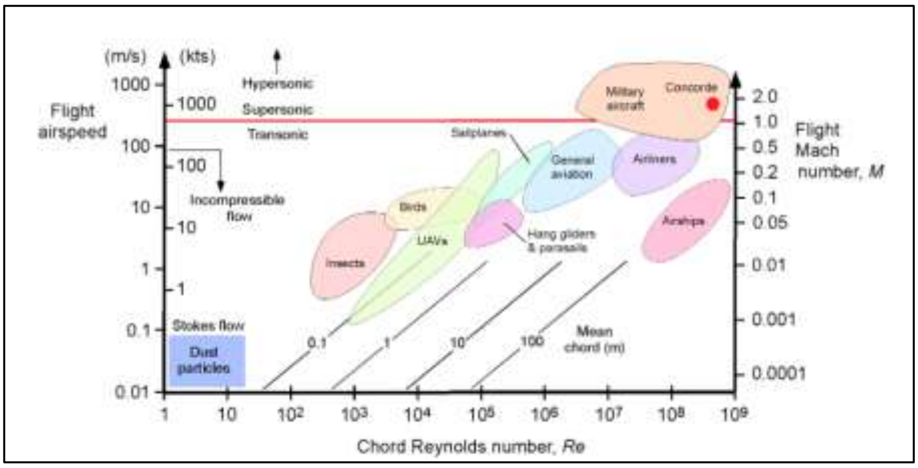

Figure 3.1: Reynolds and Mach Numbers in Diverse Flight Components [46].

a. Continuity Equation

The continuity equation is a fundamental equation in fluid mechanics that expresses mass conservation. It states that the rate at which mass enters a given volume must equal the rate at which mass leaves that volume, plus any change in the mass within the volume. This equation is used to analyse steady and unsteady flows and is written as [44]:

$$\frac{\partial \rho}{\partial t} + \nabla \cdot (\rho \text{v}) = 0 \tag{3.2}$$

whereas ρ is the density and v is the velocity vector.

b. Bernoulli's equation

Bernoulli’s equation is one of the most important equations for analysing the flow of ideal fluids (those with no viscosity and without turbulence). It describes the relationship between pressure, velocity, and height in a steady flow of a fluid and is written as [44]:

$$P + \frac{1}{2}\rho v^2 + \rho g h = \text{ constant} \tag{3.3}$$

Whereas P is the pressure, v is the velocity of the fluid, ρ is the density, g is the gravitational acceleration, and h is the height.

c. Viscosity and its Effects

Viscosity measures the internal friction between fluid layers as they move past each other. In the case of fluid flow over a solid surface, viscosity creates a boundary layer where the fluid velocity decreases gradually, eventually reaching zero at the surface due to the no-slip condition. Viscosity dissipates mechanical energy in fluid flows and plays a crucial role in analyzing viscous flows [44].

d. Velocity and Acceleration

Velocity: Velocity is a vector that defines the magnitude and direction of the movement of fluid particles at any given point. A velocity field is used to describe the behavior of fluid flow at any specific moment [44].

Acceleration: Acceleration is the rate of change of velocity with respect to time. In time-varying flows, changes in velocity affect the distribution of pressure and forces acting on the fluid, which requires the use of differential equations to describe the fluid motion accurately [44].

3.1.3 Aerodynamics Science

Aerodynamics is a branch of fluid dynamics that focuses on the study of the movement of air, particularly its interaction with solid objects such as aircraft. At the heart of aerodynamics are the forces of lift and drag, which play a crucial role in determining the performance of an object moving through the air. The science of aerodynamics encompasses various types of flow, including subsonic, transonic, supersonic, and hypersonic regimes, each with unique characteristics. It deals with both external aerodynamics, where air flows over bodies, and internal aerodynamics, concerning flows through ducts. The study involves understanding flow patterns, pressure distributions, and velocity fields, all of which are governed by fundamental principles like the conservation of mass, momentum, and energy. The Navier-Stokes equations serve as the backbone for these calculations, describing the behavior of viscous fluids. Additionally, boundary layer theory plays a critical role in explaining how air behaves close to the surface of an object, significantly impacting drag. The applications of aerodynamics range from the design of airplanes to improving the performance of automobiles, and even to wind turbines and space vehicles, making it a vital science in both engineering and physics [45].

3.1.3.1 Aerodynamics forces

a. Lift Force

Lift is the aerodynamic force generated by the pressure and shear stress distributions acting on the wing's surface. This overall force can be broken down into two components: one parallel to the relative wind and the other perpendicular to it. Drag (D) refers to the aerodynamic force component that is parallel to the relative wind, while Lift (L) is always defined as the component that is perpendicular to the relative wind. The angle formed between the relative wind and the chord line of the airfoil is known as the angle of attack (α). Lift is primarily caused by the unequal pressure distribution on the top and bottom surfaces of the airfoil. More specifically, the pressure on the upper surface is lower than that on the lower surface, creating an upward lift force. The lift can be calculated using the following equation [45]:

$$L = \frac{1}{2} \times \rho \times V^2 \times S \times C_L \tag{3.4}$$

Where:

L : Lift force.
ρ : Air density.
V : Velocity of the aircraft relative to the air
S : Wing reference area.
C_L: Lift coefficient.

The lift coefficient is calculated by dividing the aerodynamic lift by the dynamic pressure and a reference area, typically denoted as S for wings. This coefficient depends on both the Mach number (M∞) and the Reynolds number (Re), and since these quantities are dimensionless, the lift coefficient (C_L) is also dimensionless. It is derived for a particular airfoil shape at a specific angle of attack (α). If the angle of attack changes, the lift coefficient will adjust accordingly. Therefore, for a specific airfoil, the lift coefficient is influenced by the angle of attack, Mach number, and Reynolds number [45].

b. Drag Force

$$D = \frac{1}{2} \times \rho \times V^2 \times S \times C_D \tag{3.5}$$

Where:

c : Drag force.

ρ : Air density.

V : Velocity of the aircraft relative to the air

S : Wing reference area.

C_D: Drag coefficient.

The drag coefficient, C_D is a dimensionless quantity that quantifies the drag or resistance of an object in a fluid environment. It represents the drag force on an object moving through a fluid divided by the product of the fluid density, the object's reference area, and the square of the object's velocity [45].

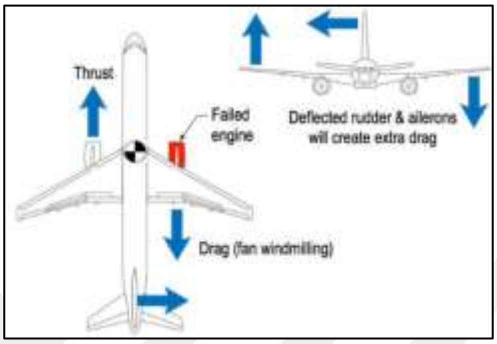

Figure 3.2: Aerodynamic Forces Acting on the Plane [47].

3.2 COMPUTATIONAL FLUID DYNAMICS

3.2.1 Introduction

Computational Fluid Dynamics (CFD) began in the early 1970s, resulting from the integration of physics, numerical mathematics, and computer science to simulate fluid flow behavior. The evolution of CFD has been closely tied to advancements in computer technology. Initially, CFD was used primarily to simulate transonic flows by solving the non-linear potential equation. In the 1980s, the ability to solve both two-dimensional and three-dimensional Euler equations emerged. With the development of supercomputers and advanced numerical techniques like multigrid, it became possible to simulate non-viscous flows around entire aircraft structures and within complex machinery. Midway through the decade, the focus shifted to more complex simulations of viscous flows, driven by the Navier-Stokes equations, alongside the rise of advanced turbulence models, such as direct numerical simulations and large eddy simulations (LES). Towards the late 1980s, real gas modeling became important, particularly for simulating three-dimensional hypersonic flows around re-entry vehicles like the European HERMES shuttle. This period also saw an emphasis on combustion simulations and flame modeling, crucial for improving gas turbines and engines with lower emissions. Grid generation methods also evolved significantly, progressing from simple structured grids to multiblock grids, grids with non-matching interfaces, and eventually the Chimera method. However, creating these detailed grids for complex geometries was time-consuming, which led to the development of unstructured grid generators and solvers for faster and more efficient setups. Today, CFD is an essential tool across various fields, including aircraft and machinery design, meteorology, oceanography, and biological research. Despite its advancements, there are still challenges to address, particularly in areas like turbulence, combustion modeling, heat transfer, and optimizing solution methods. The integration of CFD with other scientific fields, such as solid mechanics, also presents significant opportunities. This book aims to provide a solid foundation in the numerical techniques behind modern CFD, practical experience with current CFD software, and serves as a valuable resource for professionals and researchers using CFD in their work [48].

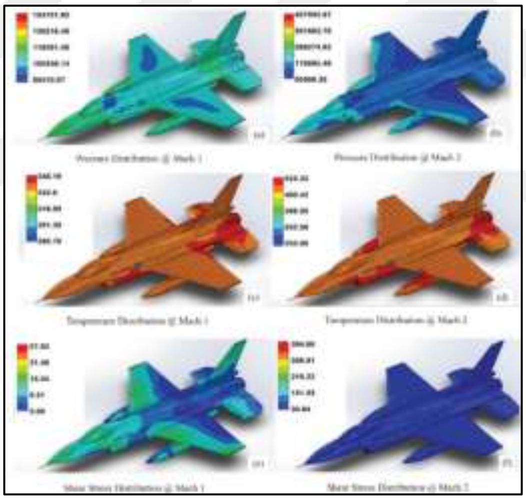

Figure 3.3: Application Using CFD Analysis [49].

3.2.2 Navier-Stokes Equations

In Computational Fluid Dynamics (CFD), especially in aerospace applications, comprehending fluid flow behaviour is essential. This behaviour is primarily governed by two key equations: the Continuity equation and the Navier-Stokes equation [50].

a. Continuity equation

Conservation of mass in fluid flow, represented as [51]:

$$\nabla \cdot u = 0 \tag{3.6}$$

b. Navier-Stokes equations [51]:

$$\frac{\partial u}{\partial t} + u\frac{\partial u}{\partial x} + v\frac{\partial u}{\partial y} = -\frac{1}{\rho}\frac{\partial p}{\partial x} + \nu\left(\frac{\partial^2 u}{\partial x^2} + \frac{\partial^2 u}{\partial y^2}\right) \tag{3.7}$$

$$\frac{\partial u}{\partial t} + u\frac{\partial v}{\partial x} + v\frac{\partial v}{\partial y} = -\frac{1}{\rho}\frac{\partial p}{\partial y} + \nu\left(\frac{\partial^2 v}{\partial x^2} + \frac{\partial^2 v}{\partial y^2}\right) \tag{3.8}$$

$$\frac{\partial u}{\partial t} + u\frac{\partial w}{\partial x} + v\frac{\partial w}{\partial y} = -\frac{1}{\rho}\frac{\partial p}{\partial z} + \nu\left(\frac{\partial^2 w}{\partial x^2} + \frac{\partial^2 w}{\partial y^2}\right) \tag{3.9}$$

whereas, the variables u, v, and w represent the velocity components in the x, y, and z directions, respectively. The symbol t stands for time, while ρ denotes the fluid density. The kinematic viscosity of the fluid is represented by ν, and p refers to the pressure field.

3.3 FLUID-STRUCTURE INTERACTION

Fluid-Structure Interaction (FSI) refers to the dynamic interplay between structures and the fluids flowing around or through them. Whether natural or engineered, structures exposed to fluid flow experience forces and vibrations caused by the movement of the fluid. These forces can lead to self-induced oscillations, known as instabilities, which are important to understand due to their potential to cause immediate damage. This book specifically examines flow-induced instabilities that occur in crossflow, where the flow moves perpendicular to the long axis of a structure. While it does not address every type of FSI, the focus is on the unique challenges and issues posed by cross-flow-induced instabilities. These instabilities are critical to a wide range of engineering applications, including heat exchangers, offshore platforms, tall buildings, and submerged pipelines. Understanding these interactions is essential for designing safe and efficient structures [52] .

One-Way FSI: In this approach, the deformations of structural elements are considered minimal and have a negligible effect on the surrounding fluid environment. As a result, the Computational Fluid Dynamics (CFD) analysis and structural analysis are treated as two independent processes, where data flows only in one direction from the fluid to the structure. The structural response is determined based solely on the fluid's pressure exerted on it, without considering how the structure's deformation might influence the fluid flow. This method is typically used for situations where structural changes are small and have an insignificant impact on the fluid, allowing such interactions to be ignored [53].

Two-Way FSI: This approach accounts for the bidirectional influence between fluid flow and structural deformation. The fluid exerts pressure on the structure, causing it to deform, which in turn alters the flow field. This mutual interaction requires an iterative exchange of data between the fluid and structural domains, with the pressure being transferred from the CFD analysis to the structural analysis, and the deformation feedback being sent back to the CFD analysis. This process continues at each step until a converged solution is reached. Two-way FSI is essential for engineering applications where the interaction between the fluid and structure significantly affects system behavior, and neglecting this mutual effect could result in inaccurate predictions [53].

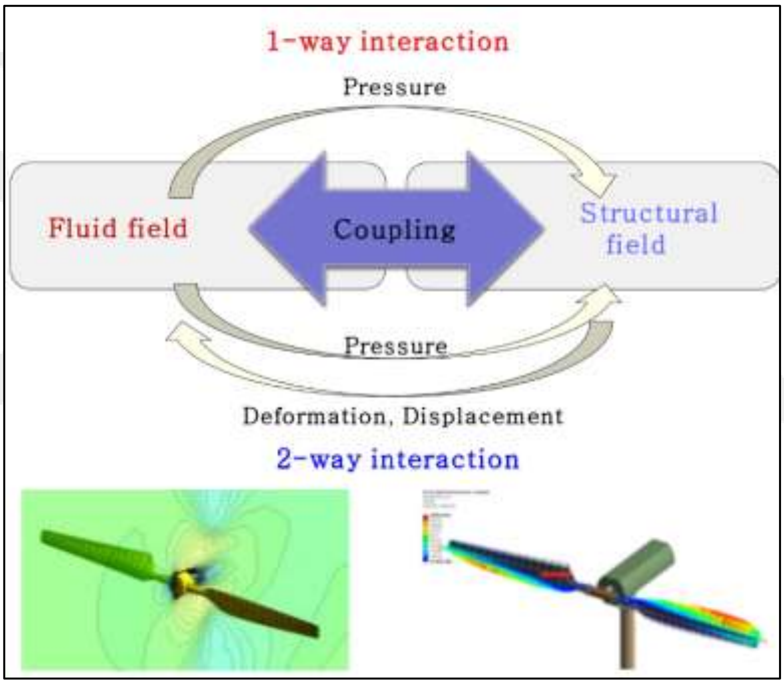

Figure 3.4: Explains One Way and Two-way FSI Analysis [54].

3.4 COMPOSITE MATERIALS

Composites are hybrid materials formed by combining at least two distinct elements, resulting in a new class of materials with unique properties. By integrating fibers or particles into organic matrices—such as polymers, metals, or ceramics—a unified material is produced that exhibits desirable traits unattainable by the individual components alone. This approach brings forth enhanced characteristics, making composites superior in certain applications compared to their separate constituents. The evolution of composite materials began with the use of larger intrinsic parts and has progressed to incorporating carbon nanotubes and nanofibers through advancements in nanotechnology. This progression has had a significant impact across various sectors, underscoring the importance of composites in modern material science. Historically present since the early days of human civilization, composites have emerged as some of the most efficient materials in contemporary engineering and technology. For example, blending epoxy resins with fibers reduces the required material dimensions while enhancing stiffness and elasticity. Advances in 3D printing technologies have further enabled the creation of composite materials that combine high strength, stiffness, low thermal expansion, thermal insulation, energy harvesting, and self-repair capabilities. These innovations not only meet complex application requirements but also open avenues in fields that demand such multifaceted properties. The development of regional materials exemplifies human ingenuity and our relentless quest to optimize the use and design of available resources. This continual improvement reflects our commitment to finding the most effective ways to harness material properties for innovative solutions [55].

3.4.1 Types of Composite Materials

a. Metal Matrix Composites (MMCs) via Powder Metallurgy Techniques

Powder Metallurgy (P/M) techniques are among the most promising methods for manufacturing Metal Matrix Composites (MMCs) MMCs are engineered materials comprising a metallic matrix reinforced with fibers that can be either ceramic or metallic. This reinforcement imparts enhanced properties to the base metal, such as increased strength, improved stiffness, and greater resistance to wear and corrosion. The fabrication of MMCs involves various manufacturing processes, including high-pressure infiltration, compression molding, vacuum infiltration molding, and pressureless metal infiltration. These composites are particularly valuable in industries that require materials to withstand high temperatures and corrosive environments. Applications are prevalent in the aerospace, automotive, and electronics sectors, utilizing materials like carbon graphite/copper, graphite/aluminum, silicon carbide (SiC)/aluminum, and SiC/magnesium composites [56].

b. Polymer Matrix Composites (PMCs)

consist of a polymer resin matrix reinforced with fibers such as glass, carbon, or aramid. These materials are distinguished by their lightweight nature, high strength, and corrosion resistance. Thermosetting polymers like epoxy and polyester provide rigidity and strength upon curing, while thermoplastic polymers such as polypropylene and nylon can be reshaped and recycled. PMCs are extensively used in the automotive, aerospace, marine, and construction industries due to their high strength-to-weight ratio and design flexibility. They are commonly employed in manufacturing vehicle body panels, structural components in aircraft, and boat construction [56].

c. Ceramic Matrix Composites (CMCs)

Ceramic Matrix Composites (CMCs) are composed of ceramic fibers embedded within a ceramic matrix. They possess high melting points, excellent thermal stability, and strong resistance to wear and corrosion, making them ideal for high-temperature applications. CMCs exhibit exceptional mechanical strength and flexibility, with service temperatures exceeding 1500°C. Owing to their ability to operate under extreme conditions, they are utilized in the aerospace industry for turbine blades, in automotive applications such as brake systems, and in the energy sector for components like heat exchanger tubes [56].

3.4.2 Integration of Composite Materials in Aerospace Applications

The advancement in manufacturing composite materials has profoundly impacted the aerospace sector, primarily due to their innovative amalgamation of high strength and superior stability with minimal weight. Structural and fiber-reinforced composites, such as Carbon Fiber-Reinforced Composites (CFRC) and Glass-Reinforced Plastic (GRP), are specifically developed to meet aerospace specifications, significantly contributing to the overall performance and efficiency of aircraft. These composites, configurable in various arrangements of their core components, find extensive use in multiple domains, including the construction of structural parts and electrical insulation. Their adaptability and resistance to adverse factors like structural fatigue and wear make them essential in modern aerospace engineering, where reducing weight must not compromise strength, durability, or corrosion resistance [57].

However, the potentially hazardous characteristics of composite materials and the associated safety risks in aerospace applications call for thorough investigation. Challenges such as delamination—where layers of laminate separate—and the potential for fiber detachment from the matrix underscore the necessity for carefully engineered and developed manufacturing technologies. The reliance on specialized equipment, like autoclaves for composite processing, significantly influences investment decisions in aerospace manufacturing technologies. Additionally, the shift from traditional materials like titanium alloys and aluminum to composites presents various difficulties, including concerns related to mechanical strength, fuel consumption, and new challenges in managing static loads, fatigue, and stress. These issues highlight the complex nature of incorporating composites into aerospace projects, requiring concerted efforts from engineers to bring these innovations to fruition while mitigating their drawbacks [57].

3.5 FREQUENCY ANALYSIS

3.5.1 Introduction

Natural frequency analysis is a vital technique used to determine the specific frequencies at which structural components naturally oscillate or resonate when subjected to external disturbances. In the context of fixed-wing UAVs (Unmanned Aerial Vehicles), numerical analysis plays a crucial role in identifying frequencies that could potentially align with operational or environmental vibrations. If these vibrations resonate with the UAV’s natural frequencies, it can lead to significant structural weaknesses, impairing performance and compromising safety. Ensuring that the UAV’s wings operate outside of these resonant frequencies is essential to prevent aerodynamic instabilities, such as flutter. Flutter is a dangerous form of oscillation that, if not controlled, can rapidly escalate, leading to destructive self-oscillation and potential structural failure [58].

3.5.2 Natural Frequency Equations

Natural Frequency General Formula [58].

$$f = \frac{1}{2\pi}\sqrt{\frac{EI}{\mu}} \tag{3.10}$$

The natural frequency (f) of a UAV wing can be determined using the following equation, where E represents the Young's modulus, reflecting the material's stiffness, I denote the second moment of inertia, indicating the wing's resistance to bending, and μ refers to the mass per unit length of the wing. This equation highlights the intrinsic relationship between the wing's vibrational characteristics and its material properties, as well as its mass distribution, underscoring the critical influence these factors have on the wing's structural dynamics [58].

3.6 KRATOS XQ-58A VALKYRIE DESIGN AND NUMERICAL ANALYSIS

3.6.1 Introduction

The XQ-58A Valkyrie is an unmanned air vehicle (UAV) developed in a collaboration between the Air Force Research Laboratory (AFRL) and Kratos Defense & Security Solutions, Inc. as part of the Low-Cost Attritable Aircraft Technology (LCAAT) program. The goal of the Valkyrie is to provide a high-performance UAV that is significantly more affordable to build and operate than traditional aircraft, whether manned or unmanned. Designed to be reusable, yet expendable in combat, the XQ-58A offers long-range, high-speed capabilities with agile maneuverability, capable of performing various missions. It is runway-independent, making it highly flexible for military operations. The UAV completed its first flight in March 2019, after only two and a half years of development from the initial contract to its inaugural flight. The XQ-58A has been undergoing continuous testing, and its future roles include acting as a communications gateway and providing low-cost forward sensing in layered defense systems. One of the key benefits of the Valkyrie is its ability to perform critical missions at a fraction of the cost of more sophisticated platforms, offering mass, complexity, and unpredictability in modern combat scenarios. The development of the XQ-58A also showcases the potential for faster, more cost-effective aircraft development by leveraging advanced design tools and commercial manufacturing processes [59].

Figure 3.5: Kratos XQ-58 Valkyrie UAV .

3.6.2 Kratos XQ-58A Valkyrie Model Design

In designing the aircraft, numerous software options were available; however, SOLIDWORKS was chosen for its user-friendly interface and the accuracy of its modeling results. The figures below illustrate the aircraft's design, with dimensions selected within the specified ranges for this type of aircraft as determined from various references.

The UAV design model is presented in the following figures.

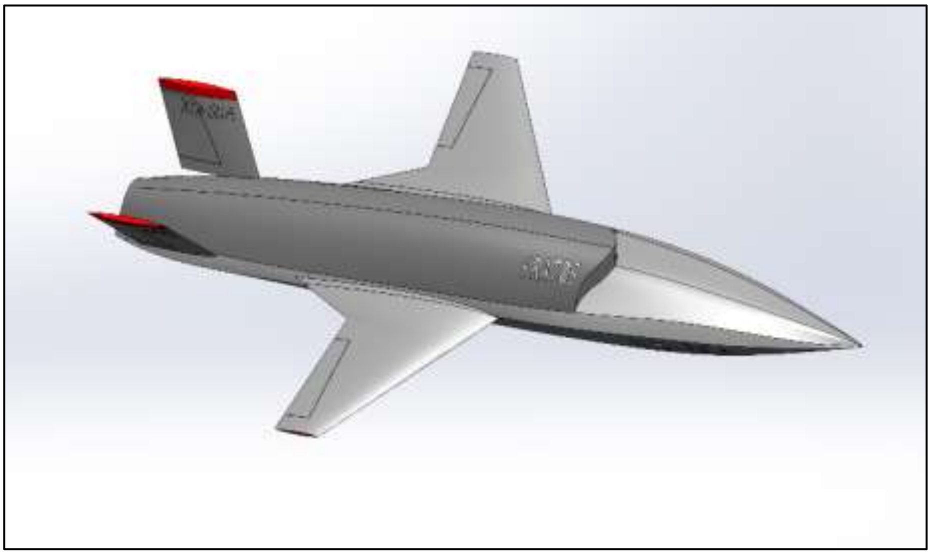

Figure 3.6: Kratos XQ-58A Valkyrie CAD Model.

Figure 3.7: Kratos XQ-58A Valkyrie Top View.

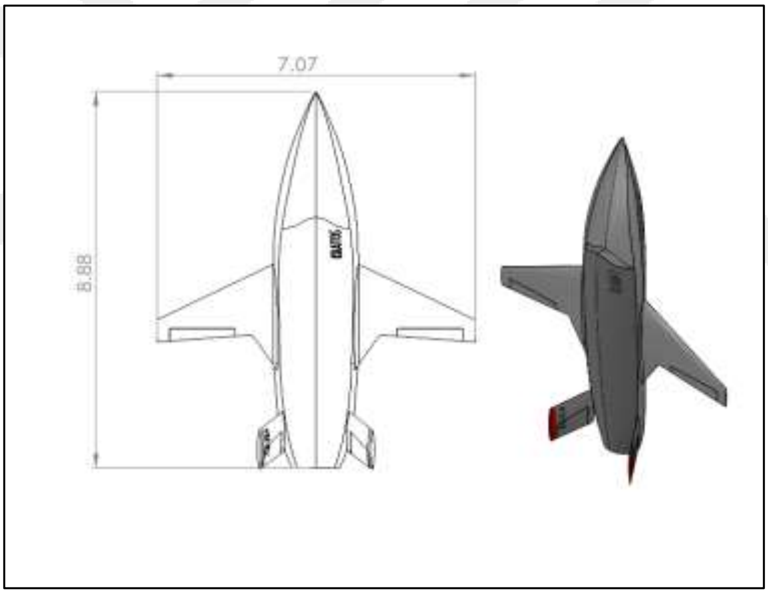

Figure 3.8: Kratos XQ-58A Valkyrie Drawing That Clarifies Dimensions.

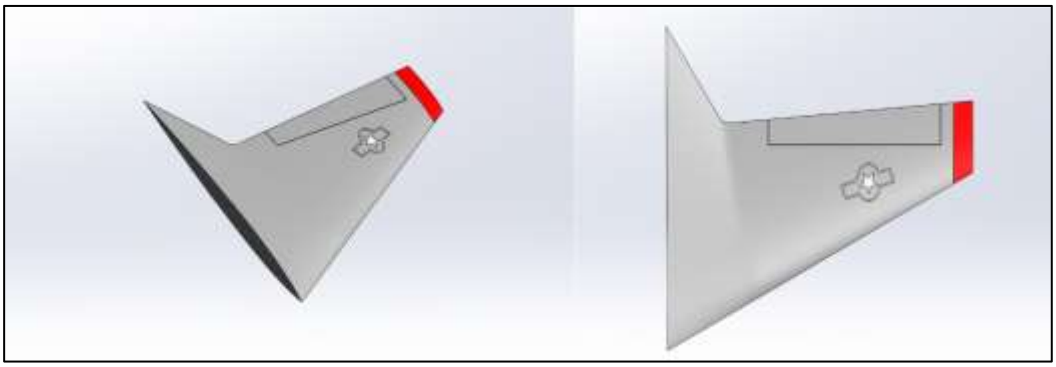

Figure 3.9: Kratos XQ-58A Valkyrie Wing.

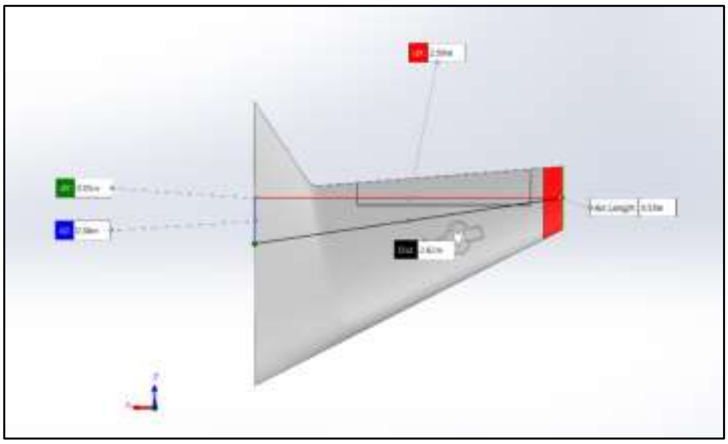

Figure 3.10: Kratos XQ-58A Valkyrie Wing Dimensions.

Table 3.1: Kratos XQ-58A Dimensions.

Parameter	**Value**
Length	11.89 m
Height	2 m
Wingspan	14.93 m
Each Wing	2.62 m

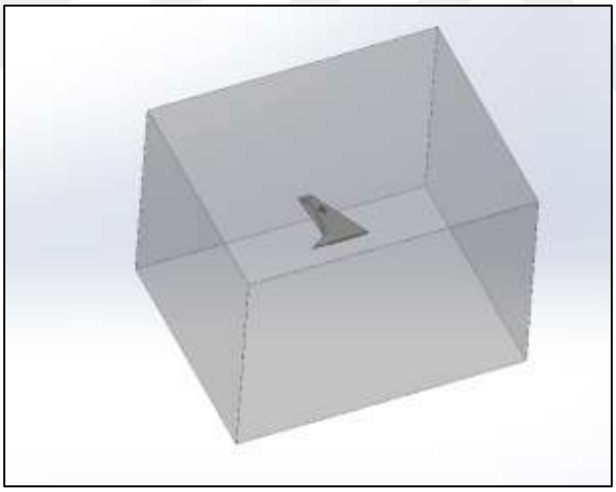

Figure 3.11: Kratos XQ-58A in Fluid Domain.

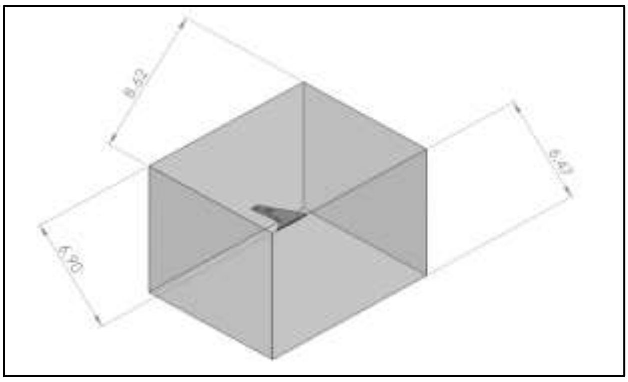

Figure 3.12: Kratos XQ-58A Fluid Domain Dimensions.

Table 3.2: Fluid Domain Properties.

Parameter	Value
Domain Length	8.62 m
Domain Width	6.90 m
Domain Hight	6.47 m

3.6.3 Kratos XQ-58 Valkyrie CFD Analysis

Upon completing the aircraft design using SOLIDWORKS, the simulation phase is conducted using ANSYS software. The UAV model is transferred to ANSYS either by exporting it in a specific file format, such as X_T, or through direct integration between SOLIDWORKS and ANSYS. Within the ANSYS Fluent environment, the geometry is imported into the computational domain. The initial step in the computational fluid dynamics (CFD) analysis involves generating the mesh of the domain, with particular emphasis on ensuring a high-quality mesh around the UAV to accurately capture the flow characteristics. The mesh settings utilized in this study are summarized in Table 3.3 below.

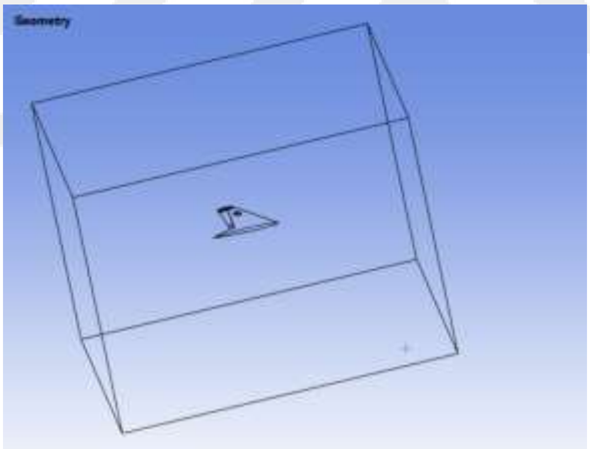

Figure 3.13 Kratos XQ-58A in ANSYS Workbench.

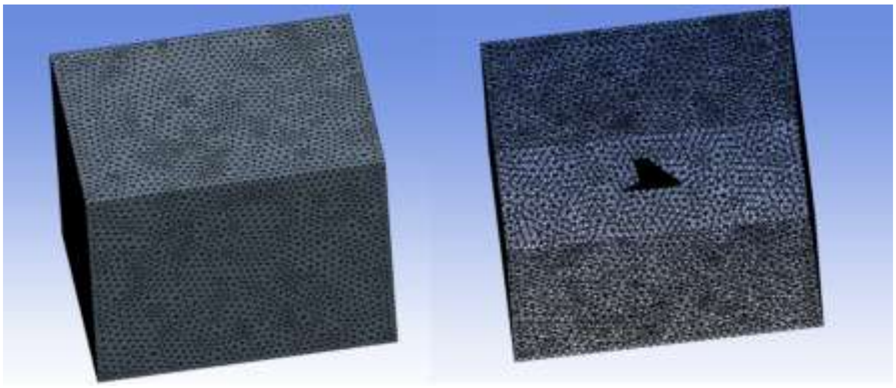

Figure 3.14: Kratos XQ-58A Fluid Domain Mesh Results.

Table 3.3: Mesh Setting in Fluid Fluent for CFD Analysis.

Parameter	Value
Method	Automatic
Sizing	100 mm

It is equally crucial to assign appropriate names to the air inlet and outlet within the defined domain, ensuring that the inlet, outlet, and the wing itself are properly labeled. The remaining sections, including the sides, top, and bottom surfaces, will be treated as walls, effectively creating a wind tunnel configuration to facilitate the completion of the analysis.

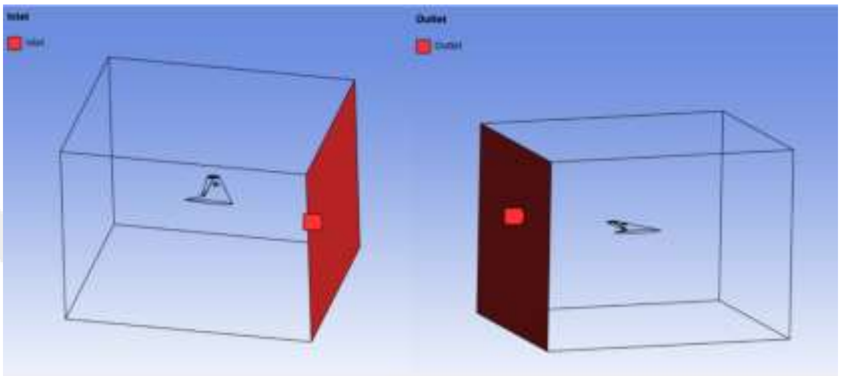

(a) (b)

Figure 3.15: Inlet and Outlet Boundary Conditions for CFD Analysis.

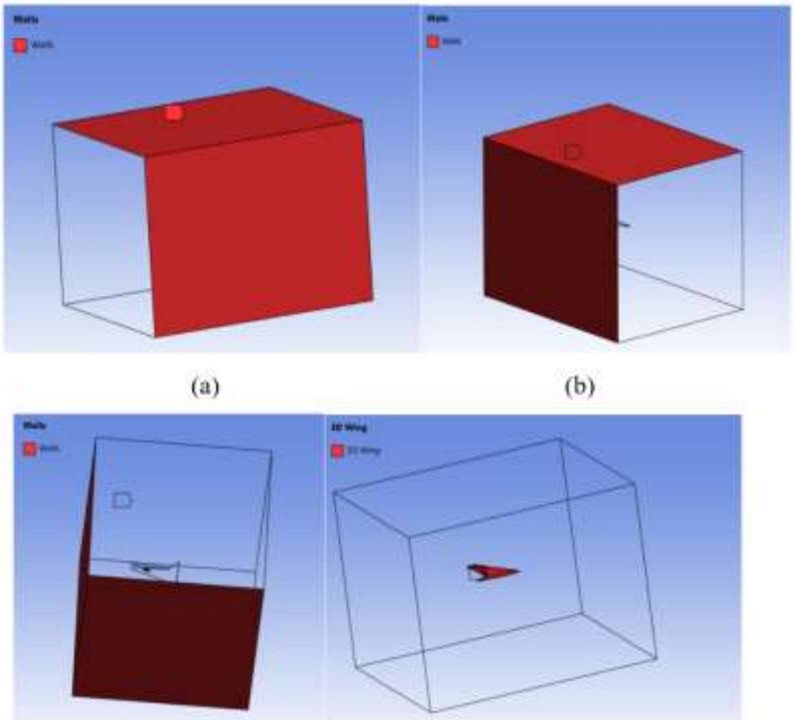

(c) (d)

Figure 3.16: All Walls and 3D Wing of Fluid Domain.

Once the meshing process is completed, the analysis will proceed based on the setup and the parameters outlined in the table below.

Table 3.4: CFD Analysis Setup Settings.

Parameter	**Value**
Study Type	Density Based
Fluid	Air
Viscous Model	k-omega (SST)
Scheme	Coupled
Flux Type	Rhie-Chow: momentum based
Pressure	Second Order
Momentum	Third-Order MUSCL
Turbulent Kinetic Energy	Third-Order MUSCL
Turbulent Dissipation Rate	Third-Order MUSCL
Iteration numbers	1000
Velocity Inlet	291.55 m/s (0.85 Mach)

3.6.4 Kratos XQ-58 Valkyrie FSI and Modal Analysis

This analysis begins after the completion of the CFD simulations, where the results from the CFD are transferred to the solid structure of the UAV. These results, specifically the pressure distribution, are imported directly into the static structural analysis. Since One-Way FSI is being used, the data flows in a single direction from the CFD analysis to the structural model, without any feedback from the structure to the fluid simulation. The aircraft's solid structure, made of aluminum, is then analyzed under these pressure loads. The same approach is applied to the airframe, which is imported into the static structural setup. The analysis begins with generating the mesh for the structure, and then the boundary conditions are defined, as shown in the tables and figures below. This process allows for efficient resource management while ensuring the accurate representation of the structural response under aerodynamic forces.

Table 3.5: Mesh Settings for FSI Analysis.

Parameter	Value
Method	Path Conforming
Sizing	70 mm

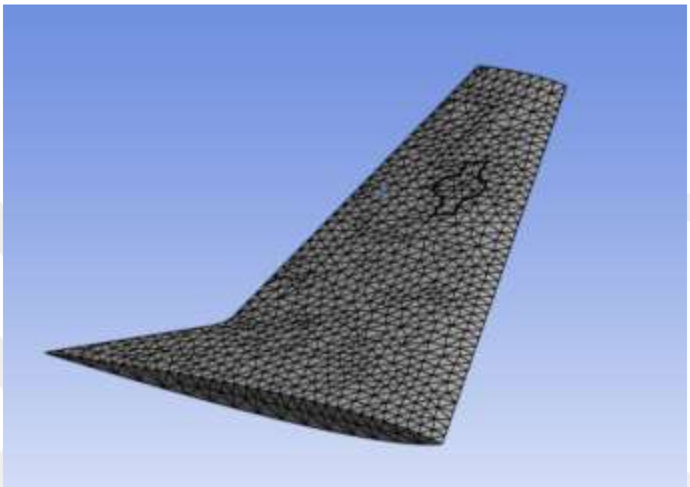

Figure 3.17: : Kratos XQ-58A Wing Mesh Results for FSI Analysis.

Since the wing is attached to the aircraft fuselage, a Fixed Support was applied as a boundary condition to the section where the wing connects to the fuselage.

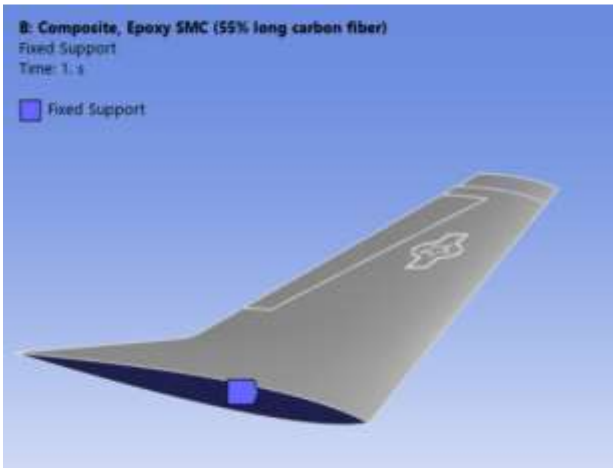

Figure 3.18: Fixed Support Boundary Condition for Kratos XQ-58A Wing.

As previously explained, and since the focus of this project is the analysis of the wing, the One-Way FSI approach was used to optimize resources and reduce time, as the primary concern is the wing's condition. After transferring the results from Fluent's fluid flow analysis to the static structural analysis window, the load value appeared as the Imported Pressure, as shown in the figure below.

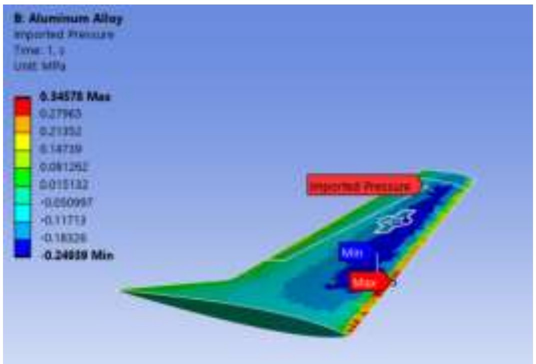

Figure 3.19: Imported Pressure (Load) on Kratos XQ-58A Wing.

As previously outlined, this research will focus on three case studies. In the first case, the traditional material used for wing construction, aluminum, will be applied. For the second and third case studies, composite materials will be utilized. The material (Epoxy SMC (65% long glass fiber)) will be used in the second case study, while (Epoxy E glass) will be applied in the third case study. The properties of these materials are detailed in the tables below.

Table 3.6: Aluminium Alloy Properties [60].

Density (kg/m³)	Young's Modulus (GPa)	Poisson's Ratio	Tensile Ultimate Strength (MPa)	Shear Modulus (GPa)	Tensile Strength (MPa)
2770	68	0.33	327	26.6	280

Table 3.7: Composite - Epoxy SMC (65% long glass fiber) Properties [61].

Density (kg/m³)	Young's Modulus (GPa)	Poisson's Ratio	Tensile Ultimate Strength (MPa)	Shear Modulus (GPa)	Tensile Strength (MPa)
1835	218.3	0.3315	353.3	81.9	224.2

Table 3.8: Composite - Epoxy E glass Properties [61].

Density (kg/m³)	Young's Modulus (GPa)	Poisson's Ratio	Tensile Ultimate Strength (MPa)	Shear Modulus (GPa)	Tensile Strength (MPa)
2000	45	0.4	1300	5	1100

After completing the analyses for the three cases, the project schematics for each scenario are illustrated in the figures below. The results from the fluid flow simulations in Fluent were coupled with the static structural analysis to map the pressure forces onto the wing, as previously explained, to determine the stresses and other relevant parameters. Subsequently, the static structural analysis was linked to the modal analysis to identify the natural frequencies of the wing in each case. The results of these analyses will be presented in the following chapter.

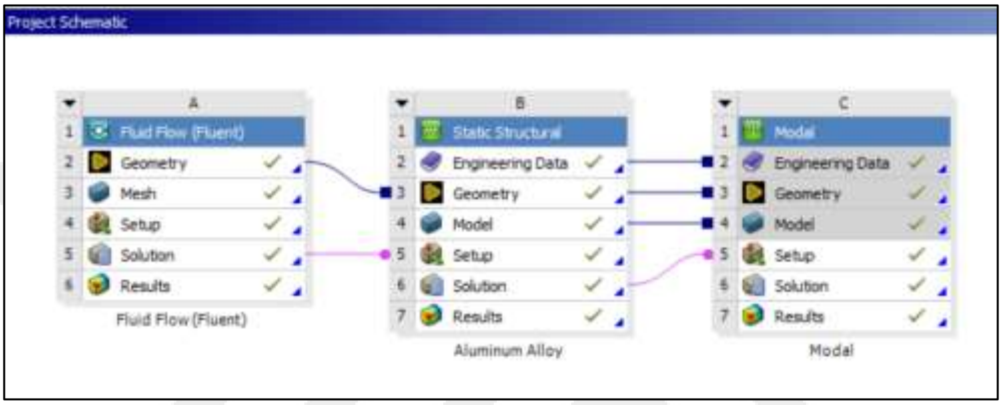

Figure 3.20: First Case Study Schematic for FSI Analysis.

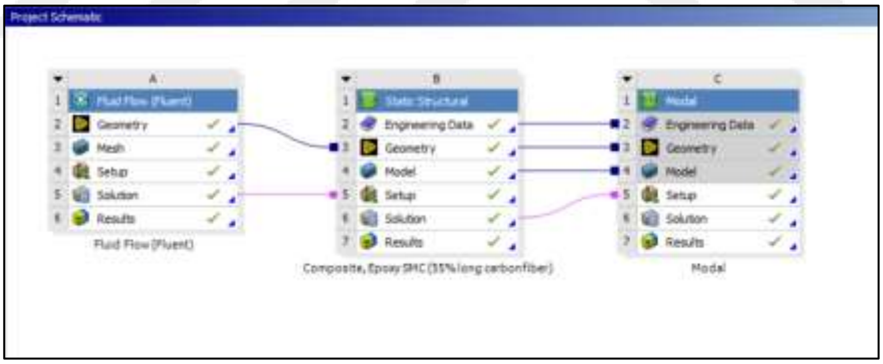

Figure 3.21: Second Case Study Schematic for FSI Analysis.

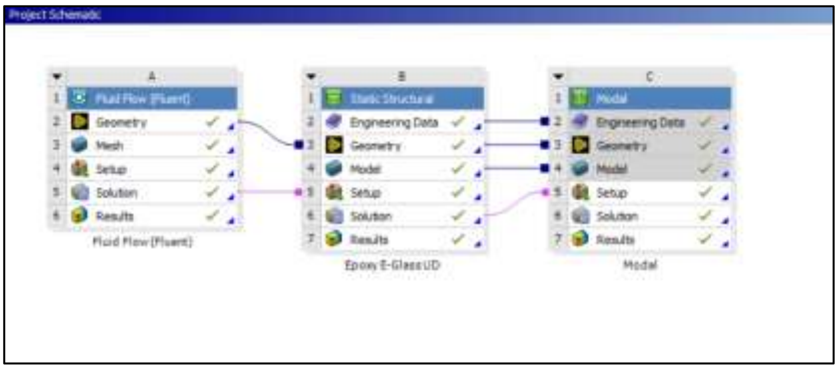

Figure 3.22: Third Case Study Schematic for FSI Analysis.

4. RESULTS AND DISCUSSION

In this chapter, the key findings from the three case studies will be presented and analysed. The three cases include the use of aluminium as the traditional material for the UAV wing, and two composite materials: Epoxy SMC (65% long glass fiber) and Epoxy E-glass. The chapter will begin by detailing the results of the CFD analysis, which is common to all three cases, as it does not depend on the material properties but rather on the aerodynamic forces acting on the wing. Following that, the results of the FSI (Fluid-Structure Interaction) and modal analysis will be presented separately for each case to assess how the different materials affect the wing's performance. This comparison will provide a clear understanding of which material offers the best performance in terms of stress, deformation, and natural frequency. Through these analyses, the chapter will evaluate which material proves to be the most effective in maintaining the structural integrity of the UAV wing under various operational conditions.

4.1 CFD ANALYSIS RESULTS

As previously explained, 1000 iterations were set for the solution process. However, the solution converged, and the process was completed by iteration 121, as shown in the scaled residuals figure below.

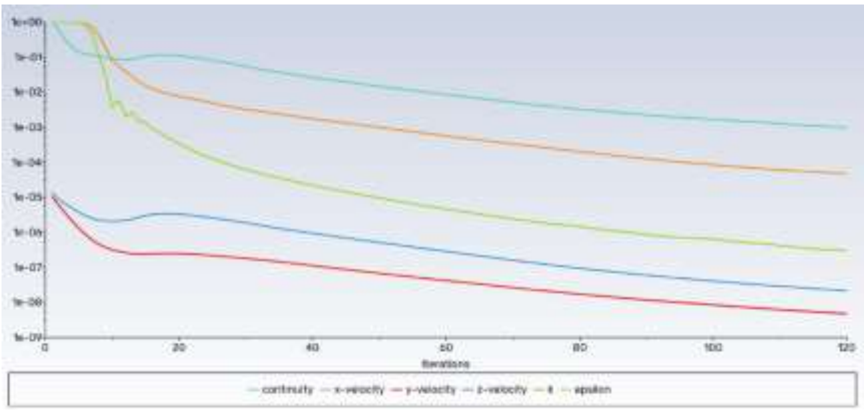

Figure 4.1: Convergence of Scaled Residuals.

4.1.1 Aerodynamics Forces,Pressures and Velocities

In the figures below, the most important contours, results, and visuals related to the lift and drag forces, their coefficients, as well as the pressure and velocity distributions on the wing of the XQ-58A Valkyrie will be displayed.

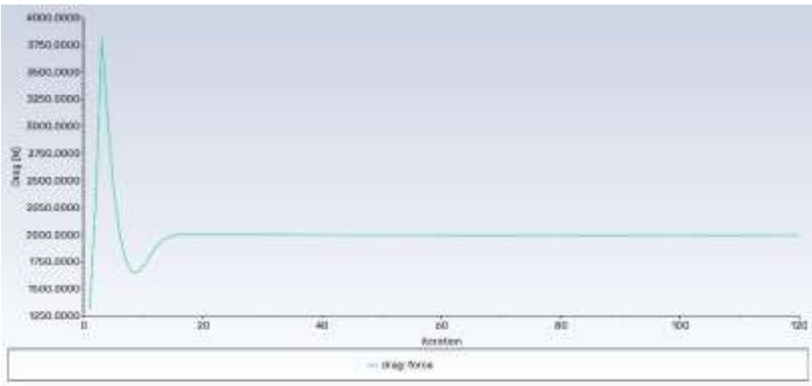

Figure 4.2: Drag Force Variation Across Iterations.

The drag force stabilized at a value of 1996.42 N.

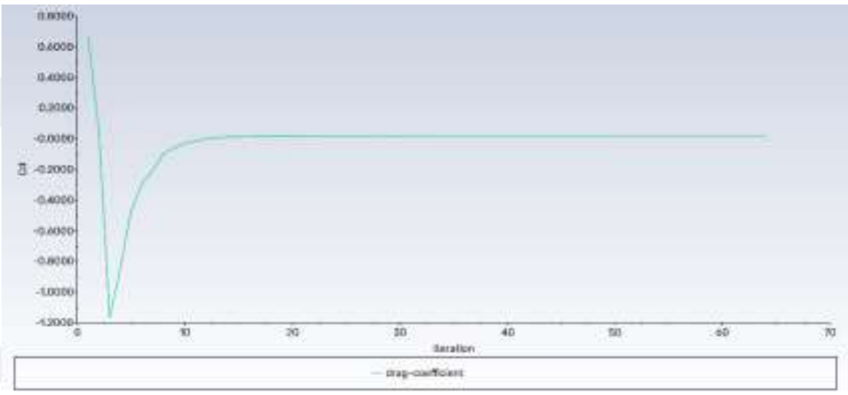

Figure 4.3: Drag Coefficient Variation Across Iterations.

The value of the drag coefficient is 0.0147.

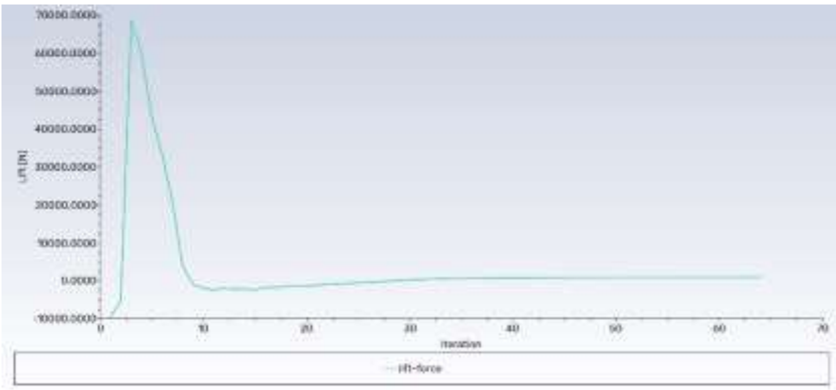

Figure 4.4: Lift Force Variation Across Iterations.

The lift force stabilized at a value of 903.58 N.

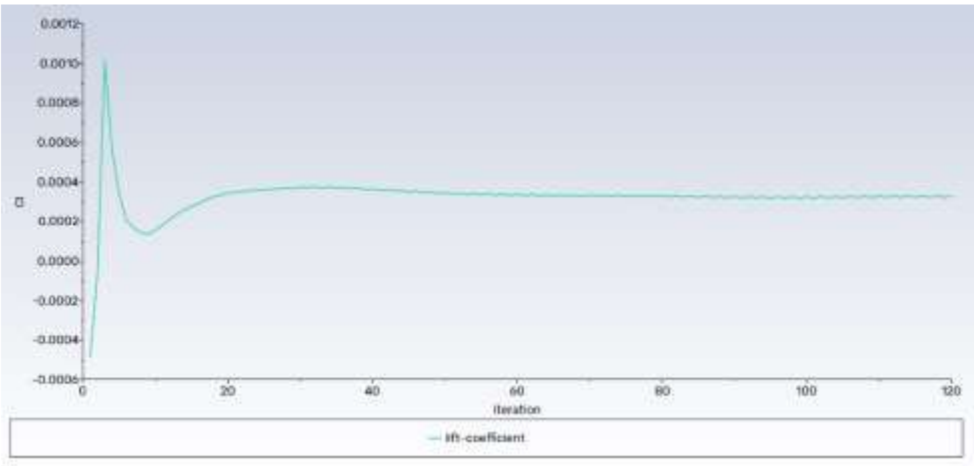

Figure 4.5: Lift Cofficent Values Vs Itarations.

The lift coefficient stabilized at a value of 0.0003.

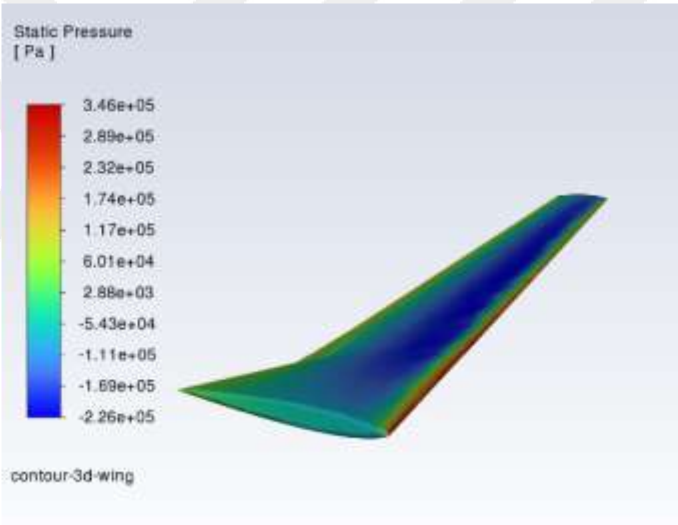

Figure 4.6: Pressure Contours on the 3D Wing of the XQ-58A Valkyrie.

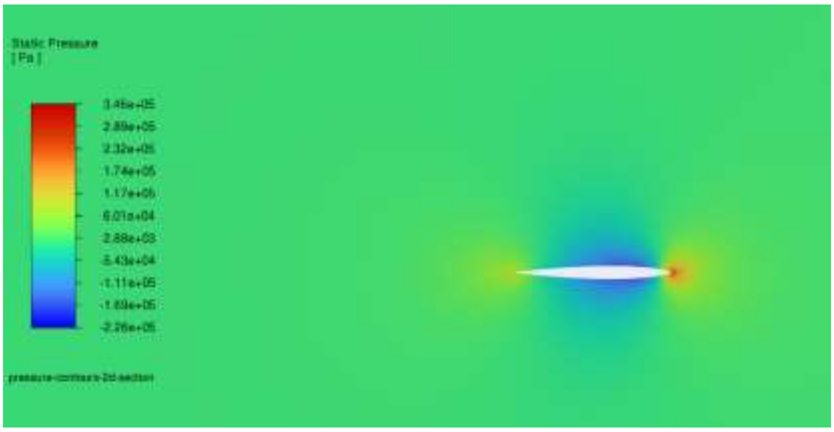

Figure 4.7: Pressure Contours on the 2D Wing Sectıon of the XQ-58A Valkyrie.

Figure 4.8: Velocity Contours on the 2D Wing Sectıon of the XQ-58A Valkyrie

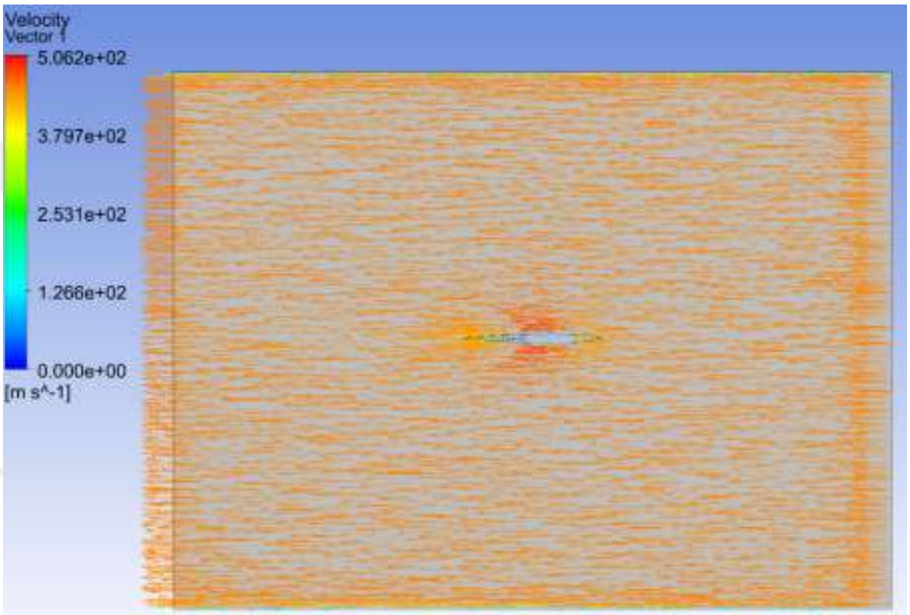

Figure 4.9: Velocity Values As Strem Lines on The Fluid Domain.

Based on the results obtained, it can be observed that as the air reaches the aircraft at maximum speed, its velocity decreases due to the collision with the aircraft, which is expected. According to Bernoulli's principle, this reduction in airspeed causes an increase in pressure. It is also noted that the pressure above the wing is generally lower (negative) compared to the higher pressure beneath the wing. This pressure difference is consistent with aerodynamic principles, as it generates the necessary lift to keep the aircraft airborne. Additionally, the lift force significantly exceeds the gravitational force, allowing the plane to maintain steady flight.

4.2 FIRST CASE STUDY RESULTS

As previously explained, the first case study focused on the wing made from aluminum, the traditional material used in its construction. First, the FSI results will be presented, followed by the modal analysis.

4.2.1 Fluid-Structure Interaction Results

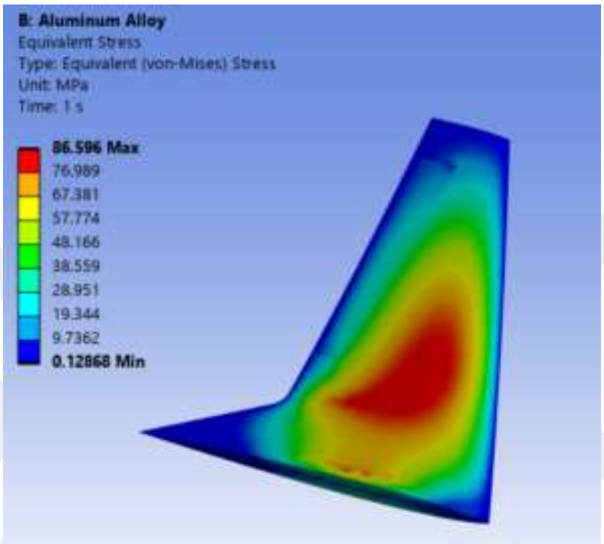

Figure 4.10: Maximum Von-Mises Stress for Alumnium Alloy Wing.

Maximum Von-Mises stress is 86.596 Mpa.

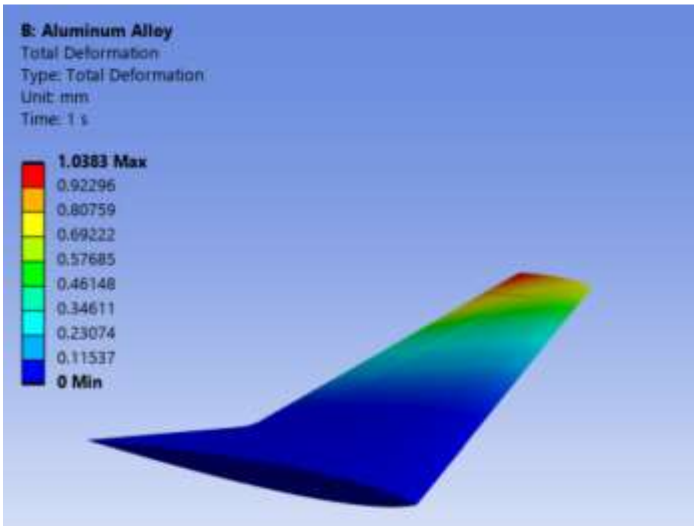

Figure 4.11: Total Deformations for Alumnium Alloy Wing.

Total Deformation is 1.0383 mm for first case study.

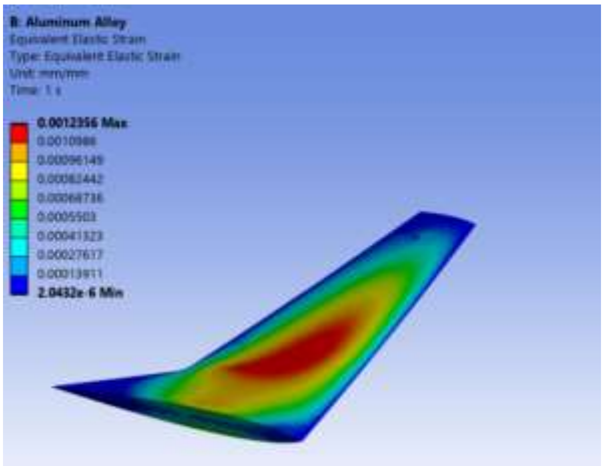

Figure 4.12: Equivelent Elastic Strain for Alumnium Alloy Wing.

The Equivalent Elastic Strain is 0.0012356 for first case study.

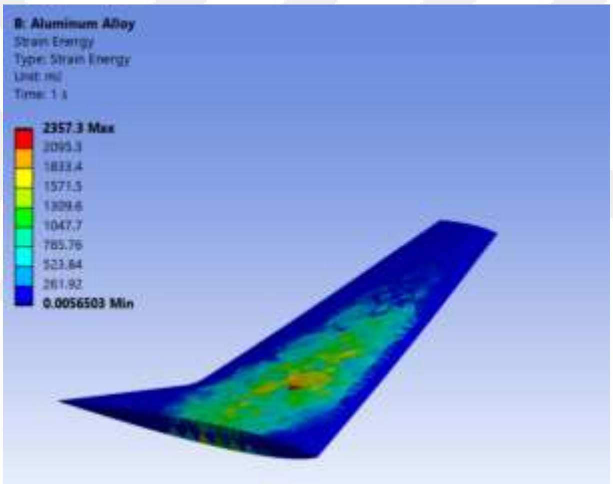

Figure 4.13: Strain Energy Values for Alumnium Alloy Wing.

The strain energy values for first case study are 2357.3 mJ.

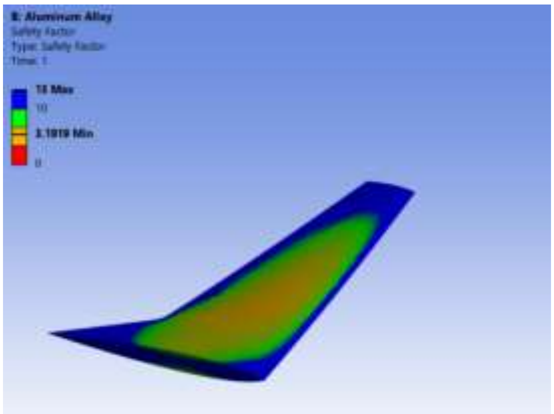

Figure 4.14: Safety Factor Values for for Alumnium Alloy Wing..

The safety factor is calculated to be 3.1919 when the aircraft wing is constructed from aluminum. Since this value is greater than 1, the structure is considered safe in this scenario.

4.2.2 Modal Analysis Results

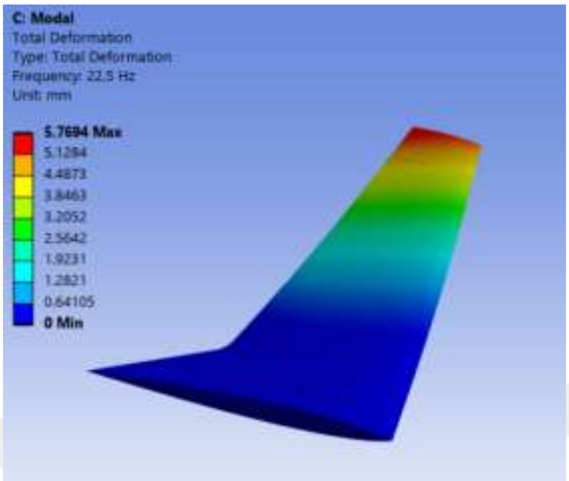

Figure 4.15: Mode 1 Result for the First Case Study.

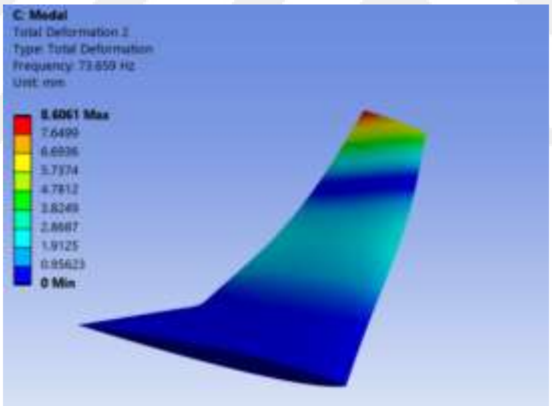

Figure 4.16: Mode 2 Result for the First Case Study.

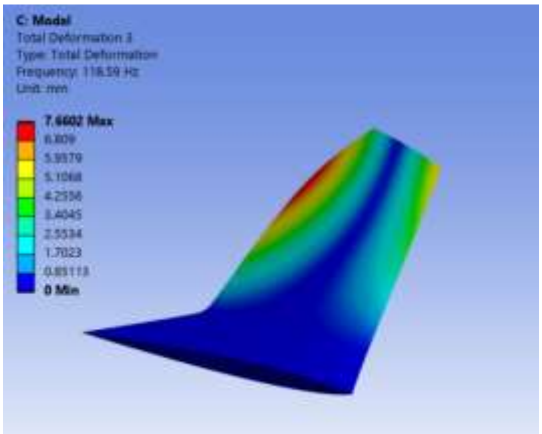

Figure 4.17: Mode 3 Result for the First Case Study.

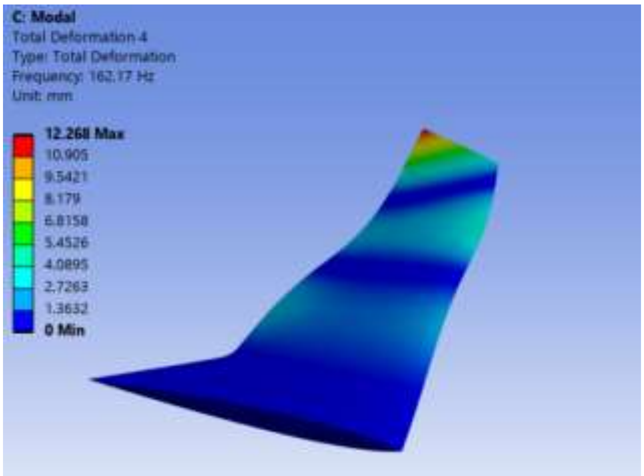

Figure 4.18: Mode 4 Result for the First Case Study.

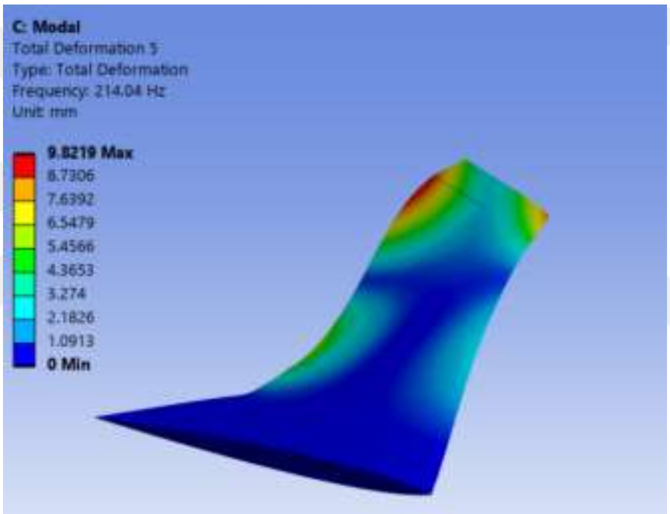

Figure 4.19: Mode 5 Result for the First Case Study.

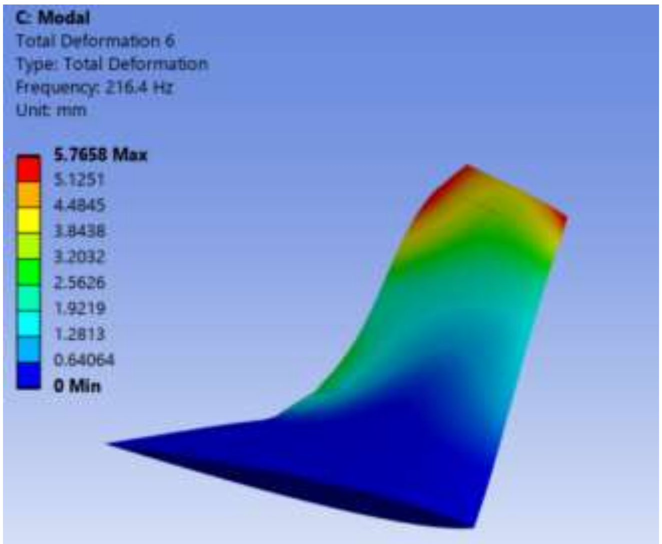

Figure 4.20: Mode 6 Result for the First Case Study.

Table 4.1: Natural Frequencies of First Case Study.

Mode	Frequency [Hz]	Total Deformation (mm)
1	22.5	5.7694
2	73.659	8.6061
3	118.59	7.6602
4	162.17	12.268
5	214.04	9.8219
6	216.4	5.7658

The results of the second case study, where **Epoxy SMC (65% long glass fiber)** was used as the material for the wing, will now be presented. The FSI and modal analysis outcomes for this case will be detailed in the following section.

4.3 SECOND CASE STUDY RESULTS

4.3.1 Fluid-Structure Interaction Results

The maximum stress results will not be presented here, as they do not depend on the type of material but rather on the magnitude of the applied forces and the wing's surface area. Since these factors remain unchanged, the result is the same as in the first case.

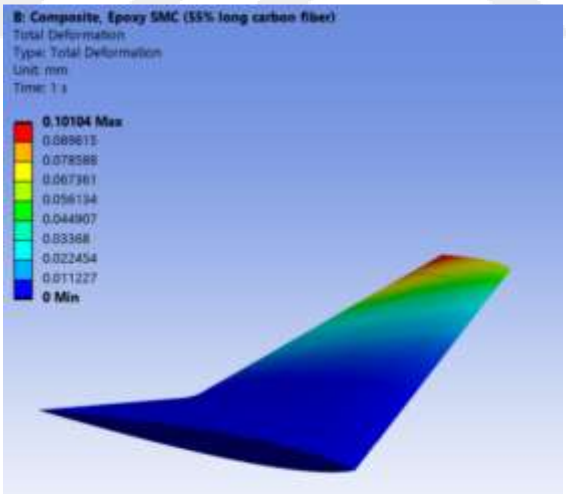

Figure 4.21: Total Deformations for Epoxy SMC (65% long glass fiber) Wing.

Total Deformation is 0.10104 mm for second case study.

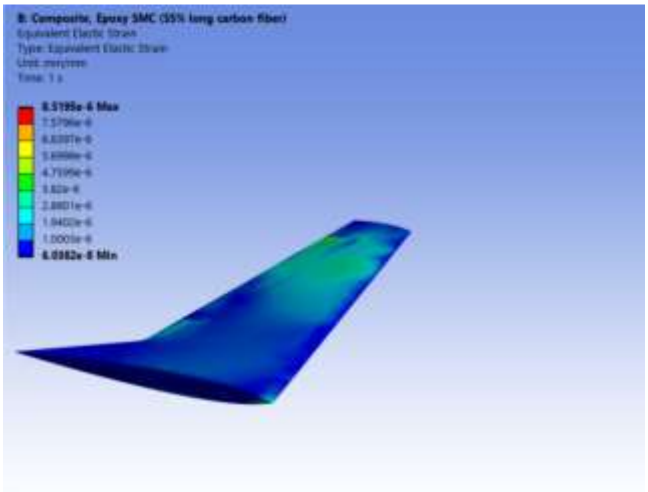

Figure 4.22: Equivelent Elastic Strain for Epoxy SMC (65% long glass fiber) Wing.

The Equivalent Elastic Strain is 0.0000085 for second case study.

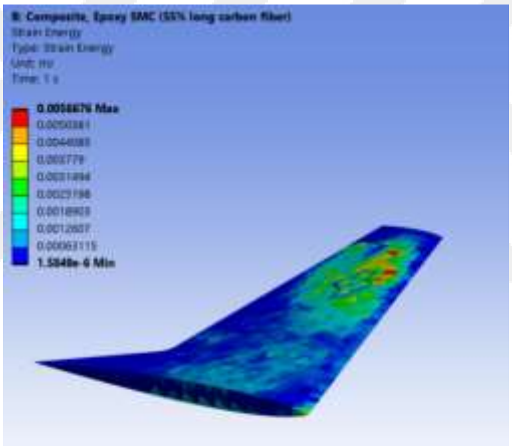

Figure 4.23: Strain Energy Values for Epoxy SMC (65% long glass fiber) Wing.

The strain energy values for second case study are 0.005667 mJ.

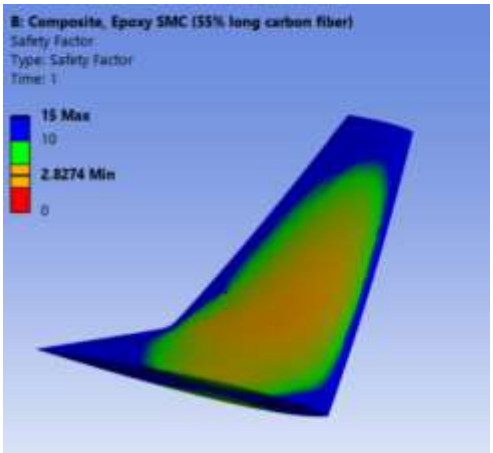

Figure 4.24: Safety Factor Values for for Epoxy SMC (65% long glass fiber) Wing.

The safety factor is calculated to be 2.8274 when the aircraft wing is constructed from Epoxy SMC (65% long glass fiber). Since this value is greater than 1, the structure is considered safe in this scenario.

4.3.2 Modal Analysis Results

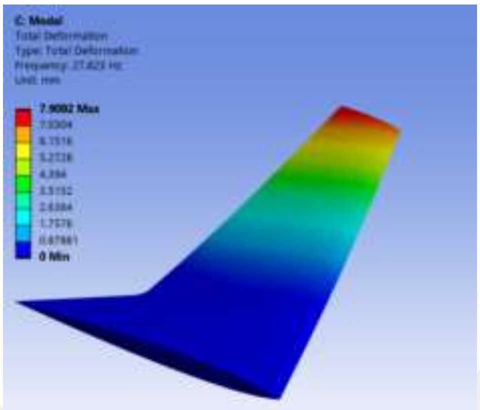

Figure 4.25: Mode 1 Result for the Second Case Study.

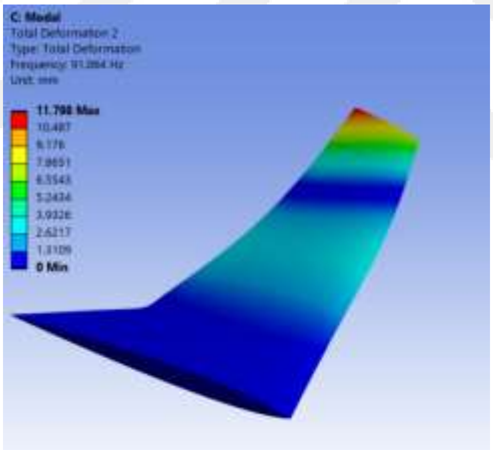

Figure 4.26: Mode 2 Result for the Second Case Study.

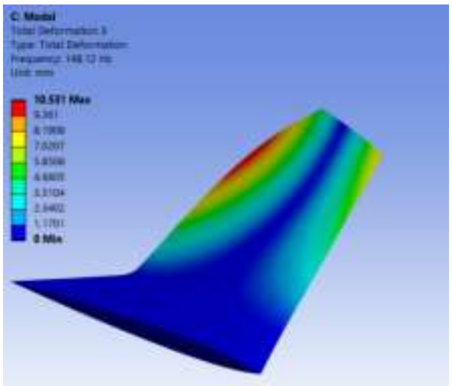

Figure 4.27: Mode 3 Result for the Second Case Study.

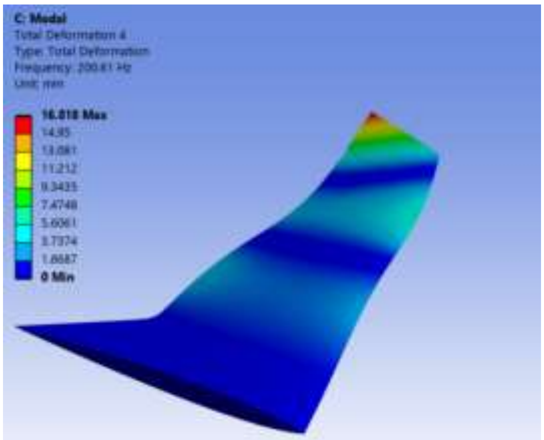

Figure 4.28: Mode 4 Result for the Second Case Study.

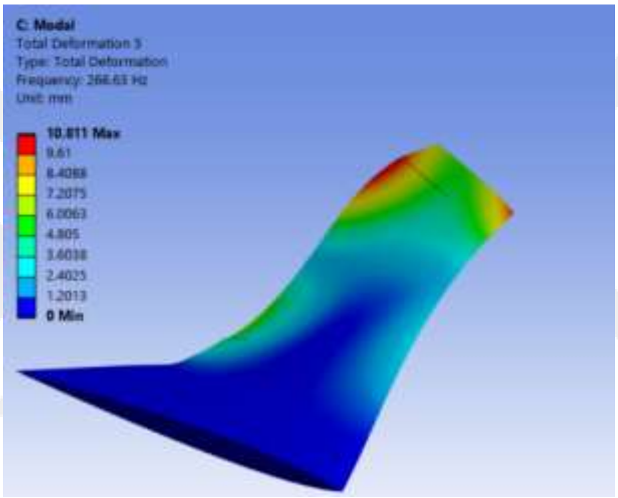

Figure 4.29: Mode 5 Result for the Second Case Study.

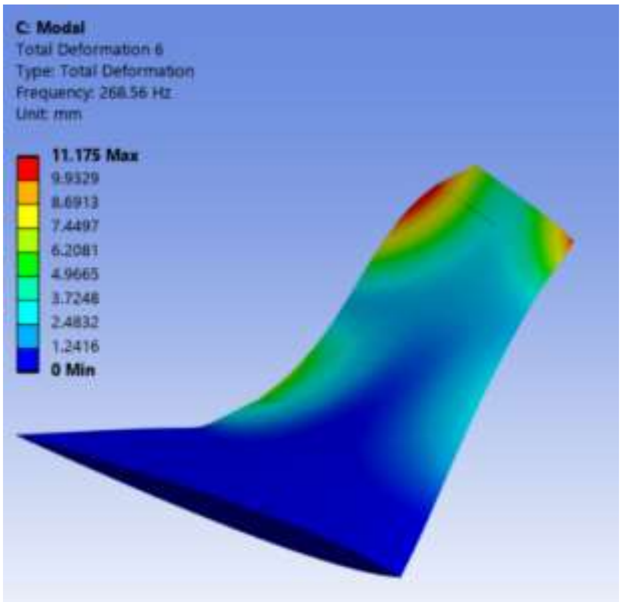

Figure 4.30: Mode 6 Result for the Second Case Study.

Table 4.2: Natural Frequencies of Second Case Study.

Mode	Frequency [Hz]	Total Deformation (mm)
1	27.823	7.9092
2	91.064	11.798
3	148.12	10.531
4	200.61	16.818
5	266.63	10.811
6	268.56	11.175

4.4 THIRD CASE STUDY RESULTS

The results of the third case study, where **Epoxy E-glass** was used as the material for the wing, will now be presented. The FSI and modal analysis outcomes for this case will be detailed in the following section.

4.4.1 Fluid-Structure Interaction Results

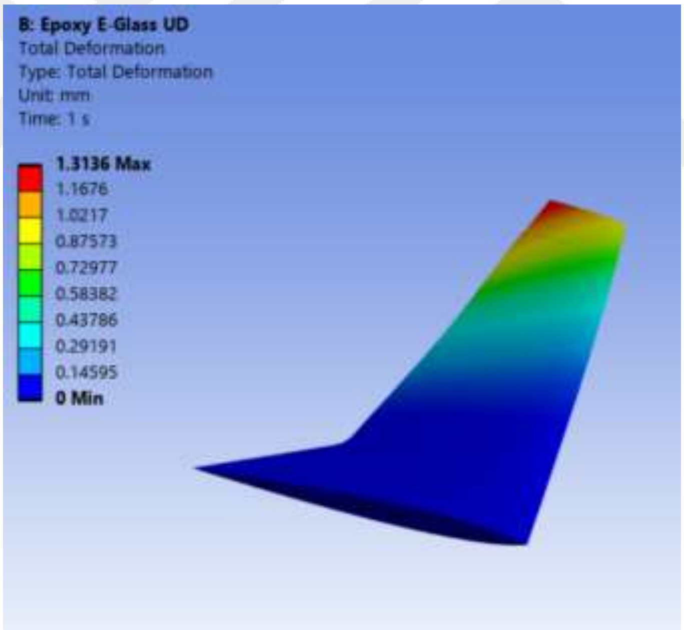

Figure 4.31: Total Deformations for Epoxy E-glass Wing.

Total Deformation is 1.31 mm for second case study.

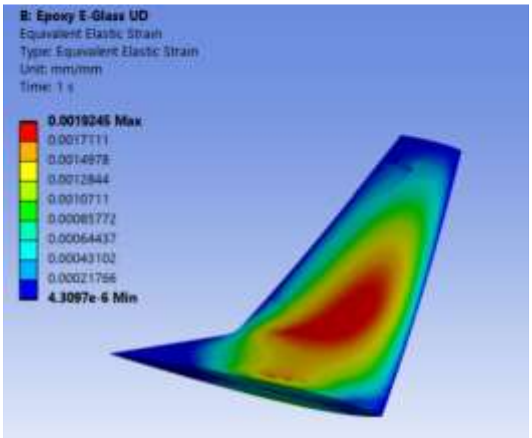

Figure 4.32: Equivelent Elastic Strain for Epoxy E-glass Wing.

Equivelent Elastic Strain is 0.00192 mm/mm for third case study.

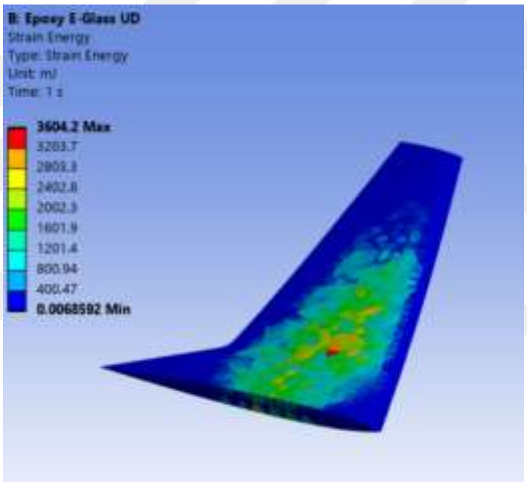

Figure 4.33: Strain Energy Values for Epoxy E-glass Wing.

The strain energy values for second case study are 3604.2 mJ.

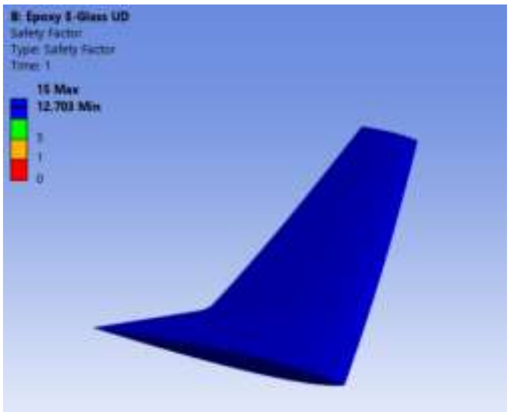

Figure 4.34: Safety Factor Values for Epoxy E-glass Wing.

The safety factor is calculated to be 12.703 when the aircraft wing is constructed from Epoxy E-glass. Since this value is greater than 1, the structure is considered safe in this scenario.

4.4.2 Modal Analysis Results

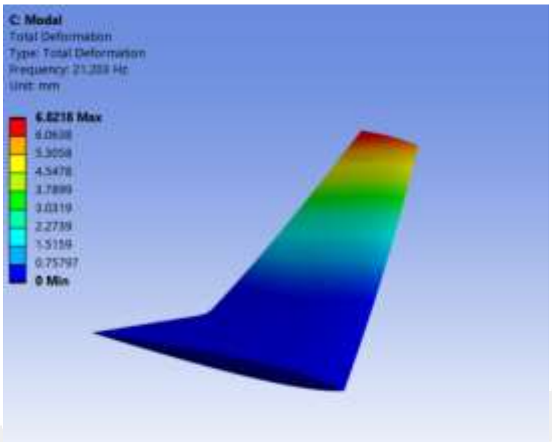

Figure 4.35: Mode 1 Result for the Third Case Study.

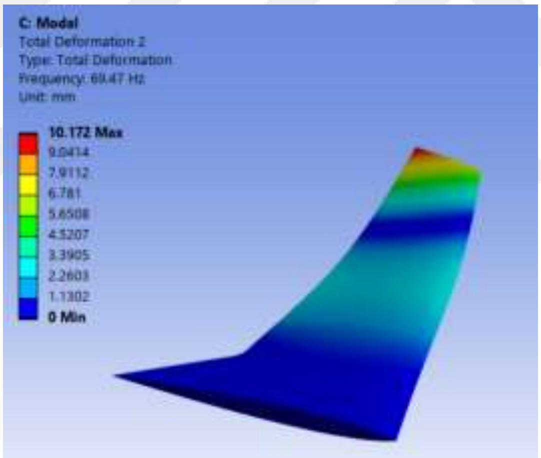

Figure 4.36: Mode 2 Result for the Third Case Study.

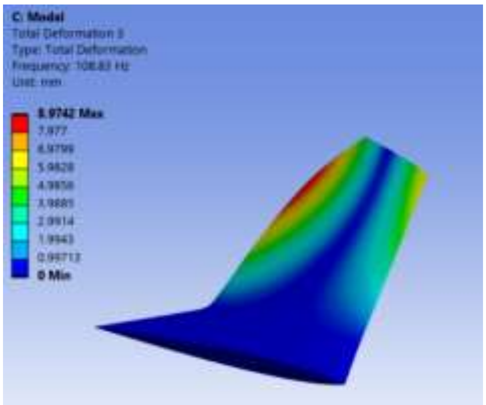

Figure 4.37: Mode 3 Result for the Third Case Study.

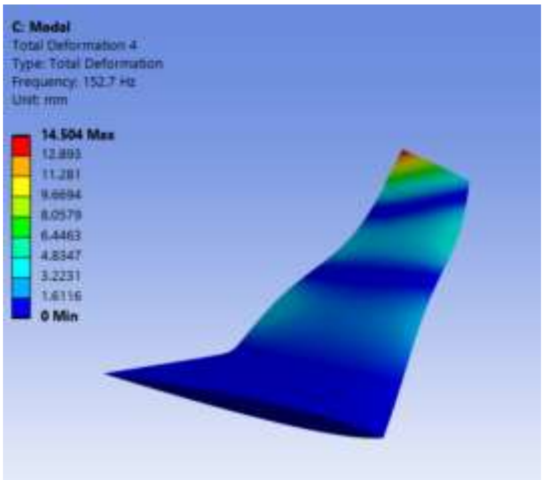

Figure 4.38: Mode 4 Result for the Third Case Study.

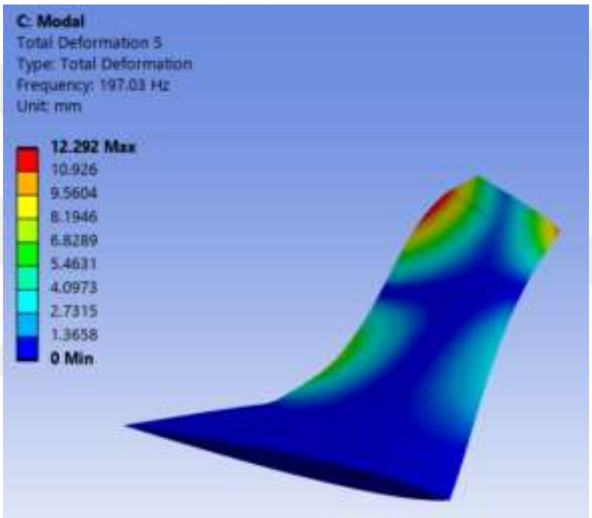

Figure 4.39: Mode 5 Result for the Third Case Study.

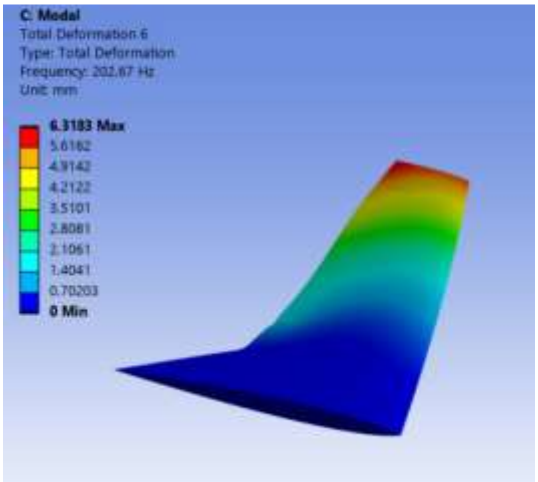

Figure 4.40: Mode 6 Result for the Third Case Study.

Table 4.3: Natural Frequencies of Third Case Study.

Mode	Frequency [Hz]	Total Deformation (mm)
1	21.203	6.82
2	69.64	10.172
3	108.83	8.9742
4	152.7	14.504
5	197.03	12.292
6	202.67	6.3183

In this study, the performance of three different materials for constructing the UAV wing was analyzed by comparing results related to deformation, strain energy, safety factor, and natural frequencies for each material. In the first case, aluminum was used as the traditional material for wing construction, while composite materials Epoxy SMC (65% long glass fiber) and Epoxy E-glass were used in the second and third case studies, respectively. This comparison aims to determine which material offers the best structural performance under various operational conditions.

First, when comparing total deformation, it is evident that Epoxy SMC exhibits the lowest deformation, at just 0.10104 mm, indicating that it provides the greatest stiffness and undergoes the least amount of displacement under load. In contrast, aluminum showed a higher deformation of 1.0383 mm, and Epoxy E-glass had the highest deformation at 1.31 mm. This suggests that Epoxy SMC offers better control over structural displacement than the other materials.

Regarding strain energy, Epoxy SMC also performed the best, absorbing the least amount of energy during deformation (0.005667 mJ), which reflects greater structural stability under applied loads. Aluminum, although showing decent performance, had significantly higher strain energy at 2357.3 mJ, but lower than Epoxy E-glass, which absorbed the most energy (3604.2 mJ). These results further support Epoxy SMC as the most efficient material in minimizing internal stress.

As for the safety factor, Epoxy E-glass demonstrated the highest value, with a safety factor of 12.703, making it the safest overall material by providing a significant margin to prevent structural failure under regular loads. Aluminum, with a safety factor of 3.1919, remains within acceptable safety limits but is lower compared to Epoxy E-glass. Epoxy SMC, while exhibiting excellent performance in terms of deformation and strain, had a lower safety factor at 2.8274, indicating that it provides a smaller safety margin under extreme operational conditions.

In terms of natural frequencies, Epoxy SMC had the highest values, making it the least prone to resonant vibrations, a phenomenon that can lead to dangerous oscillations in the aircraft structure. Epoxy E-glass, on the other hand, had the lowest natural frequencies, making it more susceptible to resonance under certain operational conditions, though this risk is mitigated by its high safety factor. Aluminum exhibited moderate performance in this category.

Based on this comparison, Epoxy SMC delivers superior performance in terms of stiffness and minimizing deformation, making it the ideal choice for applications requiring high structural stability and precise control over displacement. However, Epoxy E-glass offers the highest level of safety, making it a strong choice for applications requiring a significant safety margin, despite its greater deformation. Aluminum, while the traditional material, shows good performance but does not outperform the composite materials in most aspects.

5. CONCLUSIONS AND FUTURE WORK

5.1 CONCLUSIONS

The conclusion of this study is centered around evaluating the structural performance of a UAV wing using three different materials: traditional aluminum, Epoxy SMC (65% long glass fiber), and Epoxy E-glass. Through detailed Computational Fluid Dynamics (CFD), Fluid-Structure Interaction (FSI), and modal analysis, the study provided key insights into how each material performs under varying operational conditions.

The results demonstrated that Epoxy SMC offered superior stiffness and experienced the least deformation under load, making it an optimal choice for applications where minimizing structural displacement is critical. On the other hand, Epoxy E-glass excelled in terms of safety, with the highest safety factor, ensuring that the structure can reliably endure extreme operational conditions. Although aluminum, the traditional material, performed adequately, it did not surpass the composite materials in any significant category.

These findings underscore the potential benefits of utilizing composite materials over aluminum, particularly in UAV applications that demand structural efficiency, reduced weight, and improved safety. Epoxy SMC emerged as the best material for reducing displacement and strain on the wing, while Epoxy E-glass proved to be the safest and most reliable option. This provides valuable direction for future UAV designs, highlighting the advantages of advanced composite materials in enhancing both aerodynamic and structural performance.

5.2 FUTURE WORKS

a. Optimization of Composite Layering: Future studies should explore the use of layered composite structures to further optimize stiffness and safety. By varying the layering sequence and orientation, more efficient structural designs may be achievable.

b. Real-World Testing: While this study relied on simulation tools such as CFD and FSI, experimental validation through real-world testing of UAV wings made from these materials is essential. Physical testing would confirm the findings and account for factors that might not be captured in simulations.

c. Impact of Fatigue and Long-Term Use: Long-term structural performance under repetitive loading should be analyzed, particularly for composite materials. Understanding how Epoxy SMC and Epoxy E-glass behave under fatigue conditions could enhance their application in more demanding environments.

d. Incorporation of Advanced Aerodynamic Features: Future research could also examine the influence of advanced aerodynamic designs, such as winglets or morphing wing technology, on the overall performance when combined with these materials.

e. Exploration of Hybrid Materials: Investigating the potential for hybrid materials, combining different composites or alloys, could provide a balanced approach between stiffness, safety, and other mechanical properties.

REFERENCES

[1] M. P. Stewart and S. T. Martin, “Unmanned aerial vehicles: Fundamentals, components, mechanics, and regulations,” in *Unmanned Aerial Vehicles*, Nicholas Barrera, Ed., New York: Nova Science Publishers, 2021, ch. 1, pp. 1–70.

[2] M. Sönmez *et al.*, “Unmanned Aerial Vehicles – Classification, Types of Composite Materials Used in Their Structure and Applications,” in *ICAMS Proceedings of the International Conference on Advanced Materials and Systems*, 2022, pp. 77–82. doi: 10.24264/icams-2022.I.11.

[3] G. Nugroho, A. A. Rafsan Jani, R. R. Trio Sadewo, and M. Satrio, “Manufacturing Process and Flight Testing of an Unmanned Aerial Vehicle (UAV) with Composite Material,” *Applied Mechanics and Materials*, vol. 842, pp. 311–318, Jun. 2016, doi: 10.4028/www.scientific.net/amm.842.311.

[4] E. Esin, “VISION-AIDED LANDING FOR FIXED WING UNMANNED AERIAL VEHICLE,” MIDDLE EAST TECHNICAL UNIVERSIT, 2016. doi: 10.13140/RG.2.2.13588.09606.

[5] M. F. Soetanto and R. I. Tritjahjono, “Study the Strength of Material and Composite Structures of Belly-Landing Mini UAV,” *Applied Mechanics and Materials*, vol. 842, pp. 178–185, Jun. 2016, doi: 10.4028/www.scientific.net/amm.842.178.

[6] C. Liu, O. McAree, and W. H. Chen, “Path-following control for small fixed-wing unmanned aerial vehicles under wind disturbances,” *International Journal of Robust and Nonlinear Control*, vol. 23, no. 15, pp. 1682–1698, Oct. 2013, doi: 10.1002/rnc.2938.

[7] J. Yu, “Design and Optimization of Wing Structure for a Fixed-Wing Unmanned Aerial Vehicle (UAV),” *Modern Mechanical Engineering*, vol. 08, no. 04, pp. 249–263, 2018, doi: 10.4236/mme.2018.84017.

[8] K. N. Tahar;, A. Ahmad;, W. A. A. W. M. Akib;, and W. M. N. W. Mohd, “Aerial mapping using autonomous fixed-wing unmanned aerial vehicle,” in *IEEE 8th*

International Colloquium on Signal Processing and its Applications, IEEE, 2012, pp. 164–168. doi: 10.1109/CSPA.2012.6194711.

[9] J. Simsiriwong and R. W. Sullivan, "Vibration Testing of a Full-Scale Carbon Composite Ultralight Unmanned Aerial Vehicle," in *51st AIAA/ASME/ASCE/AHS/ASC Structures, Structural Dynamics, and Materials Conference 18th 12 - 15 April 2010, Orlando, Florida*, Aerospace research central, 2010.

[10] F. R. Triputra, R. A. S. Bambang R. Trilaksono, and M. Dahsyat, "Longitudinal Dynamic System Modeling of a Fixed-Wing UAV towards Autonomous Flight Control System Development – A Case Study of BPPT Wulung UAV Platform – ," in *2012 International Conference on System Engineering and Technology (ICSET)*, [IEEE], 2012, pp. 1–6. doi: 10.1109/ICSEngT.2012.6339294.

[11] R. Warsi Sullivan, Y. Hwang, M. Rais-Rohani, and T. Lacy, "Structural analysis and testing of an ultralight unmanned-aerial-vehicle carbon-composite wing," *J Aircr*, vol. 46, no. 3, pp. 814–820, 2009, doi: 10.2514/1.36415.

[12] W. Grodzki and A. Łukaszewicz, "Design and manufacture of umanned aerial vehicles (UAV) wing structure using composite materials," *Materwiss Werksttech*, vol. 46, no. 3, pp. 269–278, Mar. 2015, doi: 10.1002/mawe.201500351.

[13] T. SARAÇYAKUPOĞLU, H. D. DELİBAŞ, and A. D. ÖZÇELİK, "An Experimental Determination and Numerical Analysis of a Loiter Munition Unmanned Aerial Vehicle System," *International Journal of 3D Printing Technologies and Digital Industry*, vol. 6, no. 1, pp. 83–101, 2022, doi: 10.46519/ij3dptdi.1083686.

[14] A. V. Azarov, F. K. Antonov, M. V. Golubev, A. R. Khaziev, and S. A. Ushanov, "Composite 3D printing for the small size unmanned aerial vehicle structure," *Compos B Eng*, vol. 169, pp. 157–163, Jul. 2019, doi: 10.1016/j.compositesb.2019.03.073.

[15] E. I. Basri *et al.*, "Conceptual design and simulation validation based finite element optimisation for tubercle leading edge composite wing of an unmanned aerial

vehicle," *Journal of Materials Research and Technology*, vol. 8, no. 5, pp. 4374–4386, Sep. 2019, doi: 10.1016/j.jmrt.2019.07.049.

[16] C. Kim and Y. Lee, "MULTI-DISCIPLINARY DESIGN OPTIMIZATION OF UNMANNED AERIAL VEHICLE," in *Proceedings of the ASME 2011 Pressure Vessels & Piping Division Conference PVP2011 July 17-21, 2011, Baltimore, Maryland, USA*, Maryland, 2016, pp. 1–4.

[17] S. H. Son, B. L. Choi, W. J. Won, Y. G. Lee, C. W. Kim, and D. H. Choi, "Wing design optimization for a long-endurance UAV using FSI analysis and the kriging method," *International Journal of Aeronautical and Space Sciences*, vol. 17, no. 3, pp. 423–431, 2016, doi: 10.5139/IJASS.2016.17.3.423.

[18] R. Vijayakumar and S. K. Maharana, "EXPERIMENTAL CHARACTERIZATION OF GRAPHENE-BASED POLYMER MATRIX COMPOSITES FOR AN UNMANNED AERIAL VEHICLE," *International Journal of Materials Engineering and Technology*, vol. 18, no. 1, pp. 1–16, Apr. 2019, doi: 10.17654/mt018010001.

[19] C. Cruzatty, E. Sarmiento, E. Valencia, and E. Cando, "Design methodology of a UAV propeller implemented in monitoring activities," *Mater Today Proc*, vol. 49, pp. 115–121, 2022, doi: 10.1016/j.matpr.2021.07.481.

[20] B. Tamang and I. B. Ghimire, "Design And Fluid-Structure Interaction Study of a Wing Structure for a Medium-Range UAV," TRIBHUVAN UNIVERSITY, 2023.

[21] M. C. Haupt, K. Lindhorst, and P. Horst, "Interfacing MSC nastran to the CFD-Solver DLR-Tau for unsteady FSI analyses with nonlinear aircraft structures," in *AeroStruct: Enable and Learn How to Integrate Flexibility in Design*, vol. 138, 2018, pp. 155–171. doi: 10.1007/978-3-319-72020-3_10.

[22] F. life estimation of fixed-wing unmanned aerial vehicle engine by grey Forecasting, "Fatigue life estimation of fixed-wing unmanned aerial vehicle engine by grey forecasting," *Measurement and Control*, vol. 54, no. 5–6, pp. 799–810, May 2020, doi: 10.1177/0020294020915215.

[23] K. Das Patel and B. S. Kumar Karuparthi, “Design, Performance Analysis of Wing, and Manufacturing of Fixed Wing Hand Launch Unmanned Aerial Vehicle,” *International Journal of Engineering Applied Sciences and Technology*, vol. 5, no. 9, pp. 223–241, 2021, doi: 10.33564/ijeast.2021.v05i09.038.

[24] A. Felipe, C. Rivera, J. Sebastian, L. Becerra, J. Rodriguez-Ferreira, and M. Martínez, “Structural analysis of an unmanned aerial vehicle wing made of composite materials,” *Scientia et Technica*, vol. 26, no. 3, p. 13, 2021, doi: 10.22517/23447214.24535.

[25] G. Bramesfeld and R. Prinster, “Design and testing of foam-inflated wings for small unmanned aerial vehicles,” *J Unmanned Veh Syst*, vol. 3, no. 4, pp. 176–191, 2015, doi: 10.1139/juvs-2014-0018.

[26] W. Grodzki and A. Łukaszewicz, “Design and manufacture of umanned aerial vehicles (UAV) wing structure using composite materials,” *Materwiss Werksttech*, vol. 46, no. 3, pp. 269–278, Mar. 2015, doi: 10.1002/mawe.201500351.

[27] Y. Yang *et al.*, “Design, implementation, and verification of a low-cost terminal guidance system for small fixed-wing UAVs,” *J Field Robot*, vol. 38, no. 5, pp. 801–827, Aug. 2021, doi: 10.1002/rob.22012.

[28] M. El Adawy *et al.*, “Design and fabrication of a fixed-wing Unmanned Aerial Vehicle (UAV),” *Ain Shams Engineering Journal*, vol. 14, no. 9, Sep. 2023, doi: 10.1016/j.asej.2022.102094.

[29] J. H. Jang and S. H. Ahn, “Optimum Design of UAV Wing Skin Structure with a High Aspect Ratio Using Variable Laminate Stiffness,” *Applied Sciences (Switzerland)*, vol. 12, no. 19, Oct. 2022, doi: 10.3390/app12199436.

[30] M. Atmaca, B. Çetin, and E. Yılmaz, “CFD analysis of unmanned aerial vehicles (UAV) moving in flocks,” *Acta Phys Pol A*, vol. 135, no. 4, pp. 694–696, 2019, doi: 10.12693/APhysPolA.135.694.

[31] R. Warsi Sullivan, Y. Hwang, M. Rais-Rohani, and T. Lacy, “Structural analysis and testing of an ultralight unmanned-aerial-vehicle carbon-composite wing,” *J Aircr*, vol. 46, no. 3, pp. 814–820, 2009, doi: 10.2514/1.36415.

[32] F. Mazhar and A. M. Khan, “STRUCTURAL DESIGN OF A UAV WING USING FINITE ELEMENT METHOD,” in *51st AIAA/ASME/ASCE/AHS/ASC Structures, Structural Dynamics, and Materials Conference
 18th*, 2010.

[33] K. Raja Sekar, M. Ramesh, R. Naveen, M. S. Prasath, and D. Vigneshmoorthy, “Aerodynamic design and structural optimization of a wing for an Unmanned Aerial Vehicle (UAV),” in *IOP Conference Series: Materials Science and Engineering*, Institute of Physics Publishing, Mar. 2020. doi: 10.1088/1757-899X/764/1/012058.

[34] S. Rahman and A. Ranganathan, “Conceptual design and construction of a UAV wing structure,” SCI KTH, 2020.

[35] H. Sharma, C. S. Suraj, R. Antony, G. Ramesh, S. Ahmed, and P. Narayan, “Design of a High Altitude Fixed Wing Mini UAV-Aerodynamic Challenges,” *National Aerospace Laboratories Institutional Repository*, 2013.

[36] K. Das Patel and B. S. Kumar Karuparthi, “DESIGN, PERFORMANCE ANALYSIS OF WING, AND MANUFACTURING OF FIXED WING HAND LAUNCH UNMANNED AERIAL VEHICLE,” *International Journal of Engineering Applied Sciences and Technology*, vol. 5, no. 9, pp. 233–241, Jan. 2021, doi: 10.33564/ijeast.2021.v05i09.038.

[37] J. O. Imumbhon, M. Landazuri, and Y. Cao, “Structural and CFD analyses of a reciprocating-airfoil (RA) driven UAV wing under maximum lift and inertia forces,” *Drone Systems and Applications*, vol. 10, no. 1, pp. 287–308, Jan. 2022, doi: 10.1139/dsa-2021-0043.

[38] F. R. Triputra, B. R. Trilaksono, T. Adiono, R. A. Sasongko, and M. Dahsyat, “Nonlinear Dynamic Modeling of a Fixed-Wing Unmanned Aerial Vehicle: a Case Study of Wulung,” *Journal of Mechatronics, Electrical Power, and Vehicular*

Technology, vol. 6, no. 1, pp. 19–30, Jul. 2015, doi: 10.14203/j.mev.2015.v6.19-30.

[39] F. Mazhar, A. M. Khan, I. A. Chaudhry, and M. Ahsan, "On using neural networks in UAV structural design for CFD data fitting and classification," *Aerosp Sci Technol*, vol. 30, no. 1, pp. 210–225, 2013, doi: 10.1016/j.ast.2013.08.005.

[40] M. Ramesh *et al.*, "Impact behavioral studies on various composite materials using Fluid-Structure interaction (FSI)," *Mater Today Proc*, vol. 51, pp. 1134–1140, 2021, doi: 10.1016/j.matpr.2021.07.112.

[41] F. R. Triputra, B. R. Trilaksono, T. Adiono, R. A. Sasongko, and M. Dahsyat, "Nonlinear Dynamic Modeling of a Fixed-Wing Unmanned Aerial Vehicle: a Case Study of Wulung," *Journal of Mechatronics, Electrical Power, and Vehicular Technology*, vol. 6, no. 1, pp. 19–30, Jul. 2015, doi: 10.14203/j.mev.2015.v6.19-30.

[42] Z. Siddiqi and J. W. Lee, "A computational fluid dynamics investigation of subsonic wing designs for unmanned aerial vehicle application," *Proc Inst Mech Eng G J Aerosp Eng*, vol. 233, no. 15, pp. 5543–5552, 2019, doi: 10.1177/0954410019852553.

[43] R. Ramamurti, J. D. Geder, K. Viswanath, R. Lohner, and O. Soto, "Coupled CFD, Structure and Control Tool for Simulation of Flapping Wing Analysis," 2016.

[44] F. White and H. Xue, *FLUID MECHANICS*, 9th ed. New York: McGraw-Hill, 2021. [Online]. Available: https://www.mheducation.com/highered/product/fluid-mechanics-white-xue/M9781260258318.html

[45] J. D. Anderson and C. P. Cadou, *Fundamentals of Aerodynamics*, 7th ed. New York: McGraw-Hill, 2024. [Online]. Available: https://www.crcpress.com/Fundamentals-of-Picoscience/Sattler/p/book/9781466505094#googlePreviewContainer

[46] J. G. Leishman, *Introduction to Aerospace Flight Vehicles*, 1st ed. Florida: Embry-Riddle Aeronautical University, Hunt Library, 2022.

[47] E. A. Whalen *et al.*, “Full-scale Flight Demonstration of an Active Flow Control Enhanced Vertical Tail,” in *8th AIAA Flow Control Conference AIAA*, 2016, pp. 1–8. doi: 10.2514/6.2016-3927.

[48] J. BLAZEK, *Computational fluid dynamics principles and applications*. Oxford OX5: Elsevier, 2015.

[49] L. Malik and A. Tevatia, “Comparative analysis of aerodynamic characteristics of F16 and F22 combat aircraft using computational fluid dynamics,” *Def Sci J*, vol. 71, no. 2, pp. 137–145, 2021, doi: 10.14429/DSJ.71.15762.

[50] C. Pozrikidis, *Introduction to Theoretical and Computational Fluid Dynamics*. Oxford: Oxford University Press Oxford, 2011.

[51] B. R. Munson, T. H. Okiishi, W. W. Huebsch, and A. P. Rothmayer, *Fundamentals of fluid mechanics*. New York: John Wiley and Sons Inc, 2013. doi: 10.1201/b11709-7.

[52] M. P. Pa¨ıdoussis, S. J. Price, and E. de Langre, *Fluid-Structure Interactions CROSS-FLOW-INDUCED INSTABILITIES*. Cambridge: Cambridge University Press, 2010.

[53] M. Ezkurra *et al.*, “Analysis of One-Way and Two-Way FSI Approaches to Characterise the Flow Regime and the Mechanical Behaviour during Closing Manoeuvring Operation of a Butterfly Valve,” *International Journal of Mechanical and Materials Engineering*, vol. 12, no. 4, pp. 409–415, 2018, [Online]. Available: https://www.researchgate.net/publication/325170283

[54] K. Lee, Z. Huque, R. Kommalapati, and S.-E. Han, “The Evaluation of Aerodynamic Interaction of Wind Blade Using Fluid Structure Interaction Method,” *Journal of Clean Energy Technologies*, vol. 3, no. 4, pp. 270–275, 2015, doi: 10.7763/jocet.2015.v3.207.

[55] R. F. Gibson, *PRINCIPLES OF MECHANICS MATERIAL COMPOSITE*, 4th ed. Ohio: Taylor & Francis Group, LLC, 2016.

[56] G. Sumithra, R. N. Reddy, G. Dheeraj Kumar, S. Ojha, G. Jayachandra, and G. Raghavendra, "Review on composite classification, manufacturing, and applications," *Mater Today Proc*, no. xxxx, 2023, doi: 10.1016/j.matpr.2023.04.637.

[57] M. Bhong *et al.*, "Review of composite materials and applications," *Mater Today Proc*, no. June, 2023, doi: 10.1016/j.matpr.2023.10.026.

[58] N. F. Saari *et al.*, "Estimating natural frequency of pipe with various geometries: Improvement of frequency factors," *Heliyon*, vol. 10, no. 4, p. e26148, 2024, doi: 10.1016/j.heliyon.2024.e26148.

[59] K. E. Y. Benefits, "XQ-58A VALKYRIE," 2019.

[60] B. Mostefa, A. Abdelkrim, B. Ali, and B. Mohamed, "Effect of hardening induced by cold expansion on damage fatigue accumulation and life assessment of aluminum alloy 6082 T6," *Materials Research*, vol. 15, no. 6, pp. 981–985, 2012, doi: 10.1590/S1516-14392012005000123.

[61] Ansys, "Ansys Granta: Materials Information Management," ansys. [Online]. Available: https://www.ansys.com/products/materials